



Using *Daphnia* physiology to drive food web dynamics: A theoretical revisit of Lotka–Volterra models



Gurbir Perhar, Noreen E. Kelly, Felicity J. Ni, Myrna J. Simpson, Andre J. Simpson, George B. Arhonditsis *

Department of Physical and Environmental Sciences, University of Toronto, 1265 Military Trail, Scarborough, Ontario M1C 1A4, Canada

ARTICLE INFO

Article history:

Received 3 February 2016

Received in revised form 7 July 2016

Accepted 8 July 2016

Available online 9 July 2016

Keywords:

Lotka–Volterra models

Daphnia ecophysiology

Food web dynamics

Metabolomics

Prey–predator interactions

ABSTRACT

The Lotka–Volterra model is the most commonly used framework to describe the dynamics of ecological systems in which two species interact, one as a predator and the other as prey. Theoretical ecologists have since built on variants of these equations, frequently applying them to model the dynamics of algal–herbivore interactions in aquatic systems. In this study, we augment a Lotka–Volterra system by introducing a bioenergetically-explicit, ecophysiological model to examine how variations in resource allocation affect zooplankton growth and subsequently phytoplankton dynamics. Ingested material within a zooplankton's gut is separated into distinct internal congener pools that are used to support physiological processes occurring in a hierarchical direction: neurological functions, energetics, osmoregulatory maintenance, waste management, and finally growth. Consistent with the predictions of the “stoichiometric knife edge” theory, our analysis suggests that a balanced algal congener composition is required to optimize zooplankton internal congener saturations, resulting in a maximal allocation of energy to growth. In examining the advantages rendered by different strategies of minimum and optimum somatic quotas when experiencing phosphorus-enrichment conditions, we show that herbivores with narrow homeostatic bounds and animals with low minimum quotas (or depletion specialists) achieve optimal performance first. Our analysis also predicts patterns of multiple stable equilibria in which the same environmental conditions can be characterized by dramatically different prey-to-predator ratios. Importantly, abrupt shifts from one state to another can be induced not only by short-term variations in food abundance but also by variations in the nutritional quality of the prey. Our predictions have profound implications for connecting microscopic processes with macroscopic patterns and offer new insights into the multitude of factors that modulate food web dynamics.

© 2016 Elsevier B.V. All rights reserved.

1. Introduction

Lotka and Volterra's pioneering work to reproduce the dynamics of a predator–prey system has formed the core of ecological modelling over the last century (Elser et al., 2012; Wangersky, 1978). Theoretical ecologists have since built on variants of these equations, frequently applying them to model the dynamics of algal–herbivore interactions in aquatic systems. The trophic linkages between primary producers and consumers are arguably the most important in aquatic food webs (Brett and Muller-Navarra, 1997), as their interactions control the flow of energy to higher trophic levels. In freshwater pelagic environments, the keystone herbivores *Daphnia* (Altshuler et al., 2011) exert strong grazing impacts on phytoplankton biomass and species composition (Elser and Goldman, 1991; Sarnelle, 2005). The plethora of data available on *Daphnia*, spanning multiple levels of ecological organization (from genome to individuals to populations), make it a prime subject around which to develop models of food web dynamics (Mulder

and Bowden, 2007; Nisbet et al., 2010). Consequently, a rich history of *Daphnia*-based models have emerged over the past several decades that typically examine dynamics at the individual (McCauley et al., 1990; Mooij et al., 2003; Paloheimo et al., 1982; Rinke and Petzoldt, 2003) or population (McCauley et al., 1996; Nisbet et al., 1997) levels.

Contemporary zooplankton modelling has focused on internal dynamics (e.g., at the sub-individual level), investigating the theoretical implications of varying mass and energy on population dynamics and algal–herbivore interactions. For example, “ecological stoichiometry” integrates population dynamics with the mass balance of key nutrient elements, namely carbon, nitrogen, and phosphorus, in order to link grazer dynamics and algal nutritional status (Elser and Urabe, 1999; Sterner and Elser, 2002). In the last few decades, multiple stoichiometrically-explicit models of *Daphnia*–algal interactions have been developed (Andersen, 1997; Mulder and Bowden, 2007; Muller et al., 2001; Sterner, 1990), which have provided insights into the coupling of population dynamics and nutrient recycling. Further extensions of the stoichiometric concept have coupled chemical heterogeneity with Lotka–Volterra equations to capture the effects of food quality and nutrient recycling feedbacks (Andersen et al., 2004; Loladze et al.,

* Corresponding author.

E-mail address: georgea@utsc.utoronto.ca (G.B. Arhonditsis).

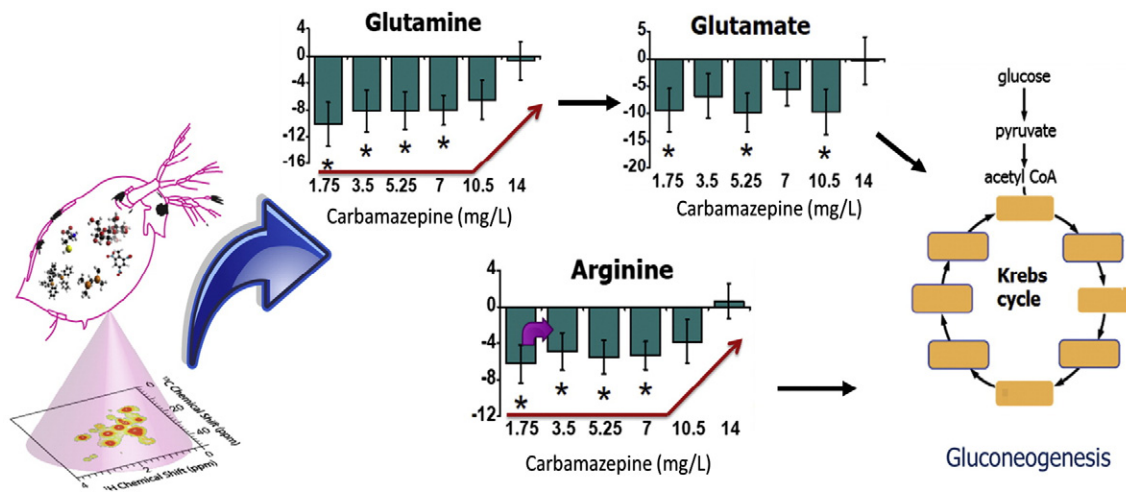


Fig. 1. Metabolomics provide metabolite-specific information regarding the perturbations of *Daphnia magna*. This illustration shows how sub-lethal carbamazepine exposure alters metabolites that participate in gluconeogenesis. Using ^1H NMR-based metabolomics, metabolite fluctuations with sub-lethal exposure can be linked to perturbations in the physiological status of *D. magna* (see Kovacevic et al., 2016 for details).

2000), while Perhar et al. (2013a) examined a zooplankton stoichiometric growth model that simulated the interplay among nitrogen, phosphorus, and highly unsaturated fatty acids (HUFAs). Stoichiometric models are now being applied to examine a phenomenon termed the “stoichiometric knife edge”, where consumer dynamics are affected by both insufficient as well as excess dietary nutrient content (Elser et al., 2012; Peace et al., 2013, 2014).

Other contemporary advances in the modelling literature have focused on energy budgets, as well as individual-based perspectives, in an attempt to introduce more realism into model dynamics. The dynamic energy budget (DEB) theory, based on a balance approach for mass and energy, seeks to capture the quantitative aspects of metabolism at the individual level for organisms of all species (Kooijman, 2010; Sousa et al., 2008). DEB models use differential equations to describe the acquisition and utilization of resources over an organism's entire life-cycle, which depend on both the state of the organism and its environment (Martin et al., 2012; Nisbet et al., 2000). For zooplankton, DEB models have successfully described growth, maturation, and reproductive processes in response to food availability (Nisbet et al., 2010), and investigated the implications of low food and starving physiology on predator-prey dynamics (Peeters et al., 2010). Individual-based models (IBMs) simulate populations composed of discrete individuals, of which each obeys a set of attributes or behaviours, such that population-level behaviours emerge from the interactions among autonomous individuals with each other and their abiotic environment (Grimm, 1999; Huston et al., 1988). This bottom-up approach can link the dynamics of individuals to higher levels of biological organization, and is thus frequently used to answer research questions that involve variations among individuals, their interactions, and individual life-cycles (DeAngelis and Grimm, 2014). Two recent studies have combined DEB theory and IBMs to predict *Daphnia* population cycles and response to toxicants (Martin et al., 2013a, 2013b).

Even though these modelling approaches collectively capture key aspects of ecosystem functioning, several limitations surrounding their use remain. For example, DEB models are attractive to ecologists because standard DEB theory is applicable across species (e.g., models differ in parameter values not mathematical structure) which offers generality, yet estimating a large number of parameters from published data to characterize the individual can be challenging (Nisbet et al., 2010; Sousa et al., 2010). Further, as the individual is the key unit of interest, extrapolating behaviour to higher levels of biological organization requires the development of additional modelling tools (Martin et al., 2012) or individual developments may not be widely applicable

to other species or ecosystem settings (DeAngelis and Grimm, 2014; but see Grimm et al., 2006, 2010). A major drawback of existing stoichiometric models is their narrow focus on nutrients as sole determinants of zooplankton growth, which does little to illuminate the broad range of daphnid internal metabolic processes. In this regard, a handful of studies have moved beyond the simple mass balance approach to incorporate separate metabolic terms for the energy and material budgets of zooplankton, in order to characterize internal homeostatic processes (Anderson et al., 2005; Arhonditsis and Brett, 2005a, 2005b; Perhar and Arhonditsis, 2012; Perhar et al., 2012, 2013b). Despite these advances, the empirical information required to properly constrain these models, as well as the sequence of physiological processes, remain poorly characterized (Perhar et al., 2013a).

An emerging field of research known as environmental metabolomics yields a promising means to depict the physiological status of zooplankton. Metabolomics is the analysis of small molecules (e.g., amino acids, proteins, carbohydrates, fats, macronutrients) within a cell, tissue, organ, biological fluid, or entire organism, in response to an external stressor (Lankadurai et al., 2013; see also our Fig. 1). Changes in organism health are manifested within the metabolome more rapidly than in the genome, proteome, and transcriptome (Viant, 2008). As a result, the field of metabolomics has emerged as a rapid, robust, and informative method for monitoring organism health (Lankadurai et al., 2013). In environmental metabolomics, nuclear magnetic resonance (NMR) is the primary platform used to identify metabolites because the non-selectivity of NMR facilitates the discovery of key metabolites that are sensitive to environmental perturbations. To date, several NMR-based metabolomic studies have successfully utilized this method to examine the response of the *Daphnia* metabolome to contaminant exposure (Li et al., 2015; Nagato et al., 2013; Poynton et al., 2011; Taylor et al., 2009, 2010; Vandenbrouck et al., 2010), although only one has examined the impact of varying nutritional sources (Wagner et al., 2015). By identifying a suite of metabolites that varied when *Daphnia* were exposed to either low food quantity, nitrogen or phosphorus limiting diets, Wagner et al. (2015) clearly demonstrated how metabolomics provide a new framework to identify the nutritional status of consumers. Combining *Daphnia* metabolomic responses into a broader modelling framework promises to rapidly accelerate our understanding of algal-grazer dynamics and unite previously discordant approaches to food web modelling.

Following this motivation, Perhar and Arhonditsis (2015) developed a bioenergetically-explicit ecophysiological model that demonstrates how variations in resource allocation affect *Daphnia* growth. This

Table 1
Modelled congeners, notations, and their functional roles in the model.

Congener	Notation (S _i)	Functional role(s)
Tryptophan	TRY	Nervous system
Tyrosine	TYR	Nervous system
Carbohydrate	CARB	Energetics
Protein	PROT	Energetics
Fat	FAT	Energetics, maintenance
Choline	CHO	Maintenance, somatic growth investment
Cholesterol	CLS	Maintenance
Eicosapentaenoic acid	EPA	Reproductive growth investment
Docosahexaenoic acid	DHA	Reproductive growth investment
Glutamic acid	GA	Waste management
Glycine	GLY	Waste management
Cysteine	CYS	Waste management
Phosphorus	P	Energetics, maintenance, somatic growth investment
Nitrogen	N	Nervous system, somatic growth investment

model tracked food particles through a zooplankter's gut, where a fraction of the grazed seston was assimilated based on its morphological characteristics, and then ingested materials were separated into distinct internal pools (termed congeners). These congener pools were used to support physiological processes occurring in a hierarchical direction: neurological functions, energetics, osmoregulatory maintenance, waste management, and finally growth. With this model, Perhar and Arhonditsis (2015) demonstrated that the elevated energetic requirements of homeostasis can significantly compromise growth when daphnids are exposed to unbalanced diets. The introduced hierarchical approach to metabolite utilization is distinct from the current elemental stoichiometric paradigm as primary regulators of algal food quality, and brings a heightened level of consumer detail to mass-balance plankton models.

Our long-term objective is to utilize *Daphnia* metabolomic data to formulate a mechanistic model that links each metabolite to one or more physiological process(es) and to shed light on the broader ecosystem implications of declining *Daphnia* health. The present study represents the second stage in which we couple the daphnid ecophysiological sub-model, developed by Perhar and Arhonditsis (2015), with a Lotka-Volterra model, depicting predator (*Daphnia*) and prey (algae) interactions. We use this model to examine three specific questions: How does varying food quality affect *Daphnia* physiological response? Which homeostatic strategy maximizes *Daphnia* physiological response to varying food quality? What are the consequences of the interplay between variations in food quality and zooplankton physiology in inducing alternative ecosystem states? The ecophysiological perspective in predator-prey models is a vital step towards connecting zooplankton dynamics with environmental signals from external stressors. As such, our goal herein is to illustrate the range of population dynamics induced when ecophysiology is explicitly considered and to project the patterns of mass and energy flow at an ecosystem scale.

2. Model description

Our model operates at two levels: the individual-based model nested within the food web model. Individual level dynamics are driven by the daphnid model developed by Perhar and Arhonditsis (2015), while the greater food web model is a modified Lotka-Volterra system, depicting the dynamics of a predator (*Daphnia*), and prey (algae). The daphnid model drives predator dynamics by modulating growth rates. Ingested matter is broken down into fourteen (14) constituent congeners. These congeners can be coarsely delineated into the following

categories (in no particular order): amino acids, highly unsaturated fatty acids (HUFAs), mineral nutrients, calorie-carrying compounds, and various other building blocks (Table 1). Congener fate within the individual's body can be either monopolized on a single, or distributed across several physiological processes. This distinction varies by both congener characteristics, and physiological systems modelled. Included in the present daphnid model are (in priority sequence): (i) neurological functions, (ii) bio-energetics, (iii) osmoregulatory and tissue maintenance, (iv) waste-management and homeostatic regulation, and (v) anabolic growth and reproductive investments. Both modelled physiological processes and the congeners driving them were devised around potentially available metabolomic lab data. This strikes a pragmatic balance for a first approximation of an explicit eco-physiological model. The modular nature of our framework not only allows for more congeners and processes to be added as new data become available, but will also allow for the incorporation of finer resolution physiological dynamics as our baseline understanding improves. Below we describe our model's physiological processes, one compartment at a time; see Table 2 for model equations, Tables S1 and S2 for parameter descriptions and values pertaining to *Daphnia* physiology, and Perhar and Arhonditsis (2015) for a fully annotated description of the model.

Our model follows a strict hierarchy, whereby physiological systems, and their respective congeners, are separated into upstream and downstream classes. The differentiating factor is their subsequent impact. Changes in upstream dynamics impart direct consequences on their downstream counterparts. These impacts can be in the forms of rate variance (e.g., bottleneck or facilitation), or logic decisions whereby the animal actively switches processes on or off. Changes in downstream processes also exert impact, but are indirect and are applied through feedback loops. Our model is designed, such that neurological functions get priority over the rest of physiological process. Driven by nitrogen (N), tryptophan (TRY), and tyrosine (TYR), this module is meant to capture the organism's nervous system robustness. Specifically, both tryptophan and tyrosine are amino acids that are present in proteins used for signal-transduction (Koide and Yoshida, 1994). Further, both amino acids are precursors to neurotransmitters (e.g., octopamine) and neurohormones (e.g., serotonin). To reflect their roles in these processes, we have exclusively tied both tryptophan and tyrosine in our model to the neurological system (i.e., they are mono-fated congeners), but have also set a small fraction of nitrogen to be used in this process. We quantify congener saturations using a modified variant of Droop's quota (Droop, 1968), whereby the internal concentration is compared against both the minimum viable concentration, and the optimum concentration (beyond which accrual can be hazardous to the individual's health). Using tryptophan and tyrosine saturations, we quantify neurological capacity by applying Liebig's law of the minimum (Liebig, 1840). That is, the least saturated neurologically-related amino acid cascades to the next physiological system: bio-energetics.

Our model considers three generic calorie-carrying compounds: carbohydrates (CARB), dietary proteins (PROT), and dietary fat (including saturated and mono-unsaturated fats; FAT). Phosphorus (P) is the fourth congener that is required for the bio-energetic compartment. Within our model, we have designated ingested carbohydrates and dietary proteins to be used exclusively for bio-energetics, but only fractions of dietary fat and phosphorus are used in this module. Calorie-carrying compounds are converted to their energetic equivalents, and summed to form the organism's potential energy. This is the energetic capacity of the individual to carry out its subsequent downstream processes under ideal circumstances. With the understanding that ideal circumstances are rarely achieved in nature, we narrow this potential energy in accordance with the previously defined neurological capacity. That is, if the least saturated neurological pool is n% saturated, the organism's energetic capacity is limited to n% of its potential energy. We refer to this constraint as the neurological bottleneck. A second bottleneck further narrows energetic capacity before it can be used to drive

Table 2
Daphnia physiology and Lotka-Volterra model equations. Definitions and values of parameters are provided in Tables S1 and S2.

Daphnia physiology sub-model equations			
1	Assimilation efficiency $AE = \frac{\alpha_{C1} \cdot F_{D1}}{\alpha_{C1} + F_{D1}}$	29	Waste management mobilization of glycine (mass) $GLY_{Mwas} = \frac{E_{WAS} \cdot WAS_{SubstL}}{GLY_{A.E.}} \cdot GLY_{SAT}$
2	Assimilated carbon $AC = graz \cdot AE$	30	Waste management mobilization of glutamic acid (mass) $GAM_{Mwas} = \frac{E_{WAS} \cdot WAS_{SubstL}}{GA_{A.E.}} \cdot GASAT$
3	Assimilated congener $ASi:C = AC \cdot food_{Si:C}$	31	Waste management mobilization of cysteine (mass) $CYS_{Mwas} = \frac{E_{WAS} \cdot WAS_{SubstL}}{CYS_{A.E.}} \cdot CYS_{SAT}$
4	Congener saturation $S_{SAT} = \frac{S_{INT} - S_{MIN}}{S_{OPT} - S_{MIN}}$	32	Energy remaining for growth $ER = EC - E_{OSM} - E_{WAS}$
5	Somatic minimum quota of congener $S_{MIN} = low \cdot S_{Som}$	33	Energy allocated to anabolic growth $E_{ANA} = ER \cdot EC_{brkd2}$
6	Somatic optimum quota of congener $S_{OPT} = high \cdot S_{Som}$	34	Energy allocated to reproductive growth $E_{REP} = ER \cdot EC_{brkd3}$
7	Neurological saturation $NEUR_{SAT} = \min(TRY_{SAT}, TYR_{SAT})$	35	Division of energy (anabolic growth) $ANA_{brkd} = [P, N, CLS]$
8	Neurological mobilization of tryptophan (mass) $TRY_{Mneuro} = TRY_{INT} \cdot TRY_{SAT} \cdot NeuroRate$	36	Anabolic growth mobilization of phosphorus (mass) $P_{Mana} = \frac{E_{ANA} \cdot ANA_{brkd1}}{P_{A.E.}} \cdot P_{SAT} \cdot P_{ANA}$
9	Neurological mobilization of tyrosine (mass) $TYR_{Mneuro} = TYR_{INT} \cdot TYR_{SAT} \cdot NeuroRate$	37	Anabolic growth mobilization of nitrogen (mass) $N_{Mana} = \frac{E_{ANA} \cdot ANA_{brkd2}}{N_{A.E.}} \cdot N_{SAT} \cdot N_{ANA}$
10	Neurological mobilization of nitrogen (mass) $N_{Mneuro} = N_{INT} \cdot N_{NEURO} \cdot NeuroRate$	38	Anabolic growth mobilization of cholesterol (mass) $CLS_{Mana} = \frac{E_{ANA} \cdot ANA_{brkd3}}{CLS_{A.E.}} \cdot CLS_{SAT} \cdot CLS_{ANA}$
11	Energetic mobilization of carbohydrates (mass) $CARB_{MOBM} = NEUR_{SAT} \cdot CARB_{INT} \cdot MobRate$	39	Division of energy (reproductive growth) $REP_{brkd} = [EPA, DHA]$
12	Energetic mobilization of carbohydrates (energy) $CARB_{MOBE} = CARB_{MOBM} \cdot CARB_{YIELD}$	40	Reproductive growth mobilization of EPA (mass) $EPA_{Mrep} = \frac{E_{REP} \cdot REP_{brkd1}}{EPA_{A.E.}} \cdot EPA_{SAT}$
13	Energetic mobilization of fats (mass) $FAT_{MOBM} = NEUR_{SAT} \cdot FAT_{INT} \cdot FAT_{ENERGY} \cdot MobRate$	41	Reproductive growth mobilization of DHA (mass) $DHA_{Mrep} = \frac{E_{REP} \cdot REP_{brkd2}}{DHA_{A.E.}} \cdot DHA_{SAT}$
14	Energetic mobilization of fats (energy) $FAT_{MOBE} = FAT_{MOBM} \cdot FAT_{YIELD}$	42	Realized growth $G = G_{max} \cdot \left(\frac{E_{ANA} + E_{REP}}{E_{ANA} + E_{REP} + E_{Os}} \right)$
15	Energetic mobilization of proteins (mass) $PROT_{MOBM} = NEUR_{SAT} \cdot PROT_{INT} \cdot MobRate$	43	Tryptophan governing equation $\frac{dTRY_{INT}}{dt} = A_{TRY:C} - TRY_{Mneuro} - T_{TRY:C} - TRY_{INT} \cdot G$
16	Energetic mobilization of proteins (energy) $PROT_{MOBE} = PROT_{MOBM} \cdot PROT_{YIELD}$	44	Tyrosine governing equation $\frac{dTYR_{INT}}{dt} = A_{TYR:C} - TYR_{Mneuro} - T_{TYR:C} - TYR_{INT} \cdot G$
17	Energetic mobilization of phosphorus (mass) $P_{MOBM} = P_{INT} \cdot P_{ENERGY} \cdot MobRate$	45	Carbohydrates governing equation $\frac{dCARB_{INT}}{dt} = A_{CARB:C} - CARB_{MOBM} - T_{CARB:C} - CARB_{INT} \cdot G$
18	Total energetic capacity $EC = (CARB_{MOBE} + FAT_{MOBE} + PROT_{MOBE}) \cdot P_{SAT} \cdot P_{ENERGY}$	46	Fats governing equation $\frac{dFAT_{INT}}{dt} = A_{FAT:C} - (FAT_{MOBM} + FAT_{Mosm}) - T_{FAT:C} - FAT_{INT} \cdot G$
19	Division of total energetic capacity $EC_{brkd} = [OSM, ANA, REP]$	47	Proteins governing equation $\frac{dPROT_{INT}}{dt} = A_{PROT:C} - PROT_{MOBM} - T_{PROT:C} - PROT_{INT} \cdot G$
20	Energy allocated to osmoregulatory maintenance $E_{OSM} = EC \cdot EC_{brkd1}$	48	Nitrogen governing equation $\frac{dN_{INT}}{dt} = A_{N:C} - (N_{Mneuro} + N_{Mana}) - T_{N:C} - N_{INT} \cdot G$
21	Division of energy (osmoregulatory maintenance) $OSM_{brkd} = [P, CHO, CLS, FAT]$	49	Phosphorus governing equation $\frac{dP_{INT}}{dt} = A_{P:C} - (P_{MOBM} + P_{Mosm} + P_{Mana}) - T_{P:C} - P_{INT} \cdot G$
22	Osmoregulatory mobilization of phosphorus (mass) $P_{Mosm} = \frac{E_{OSM} \cdot OSM_{brkd1}}{P_{A.E.}} \cdot P_{SAT} \cdot P_{MAINT}$	50	Cholesterol governing equation $\frac{dCLS_{INT}}{dt} = A_{CLS:C} - (CLS_{Mosm} + CLS_{Mana}) - T_{CLS:C} - CLS_{INT} \cdot G$
23	Osmoregulatory mobilization of choline (mass) $CHO_{Mosm} = \frac{E_{OSM} \cdot OSM_{brkd2}}{CHO_{A.E.}} \cdot CHO_{SAT}$	51	Choline governing equation $\frac{dCHO_{INT}}{dt} = A_{CHO:C} - CHO_{Mosm} - T_{CHO:C} - CHO_{INT} \cdot G$
24	Osmoregulatory mobilization of cholesterol (mass) $CLS_{Mosm} = \frac{E_{OSM} \cdot OSM_{brkd3}}{CLS_{A.E.}} \cdot CLS_{SAT} \cdot CLS_{MAINT}$	52	EPA governing equation $\frac{dEPA_{INT}}{dt} = A_{EPA:C} - EPA_{Mrep} - T_{EPA:C} - EPA_{INT} \cdot G$
25	Osmoregulatory mobilization of fats (mass) $FAT_{Mosm} = \frac{E_{OSM} \cdot OSM_{brkd4}}{FAT_{A.E.}} \cdot FAT_{SAT} \cdot FAT_{MAINT}$	53	DHA governing equation $\frac{dDHA_{INT}}{dt} = A_{DHA:C} - DHA_{Mrep} - T_{DHA:C} - DHA_{INT} \cdot G$
26	Energy allocated to waste management $E_{WAS} = E_{OSM} + \sum E_{TSi:C}$	54	Glycine governing equation $\frac{dGLY_{INT}}{dt} = A_{GLY:C} - GLY_{Mwas} - T_{GLY:C} - GLY_{INT} \cdot G$
27	Division of energy (waste management) $WAS_{brkd} = [GLY, GA, CYS]$	55	Glutamic acid governing equation $\frac{dGA_{INT}}{dt} = A_{GA:C} - GA_{Mwas} - T_{GA:C} - GA_{INT} \cdot G$
28	Turnover of excess congeners (recycled mass and associated energy) $T_{Si:C} = \frac{top \cdot (EC - E_{OSM} - E_{WAS}) \cdot \left(\frac{S_{INT} - S_{OPT}}{S_{OPT}} \right)}{\sum \left(\frac{S_{INT} - S_{OPT}}{S_{OPT}} \right) \cdot S_{iA.E.}} \cdot e^b \cdot e^{-\left(\frac{S_{INT} - S_{OPT}}{S_{OPT}} \right)}$ $E_{TSi:C} = \frac{top \cdot (EC - E_{OSM} - E_{WAS}) \cdot \left(\frac{S_{INT} - S_{OPT}}{S_{OPT}} \right)}{\sum \left(\frac{S_{INT} - S_{OPT}}{S_{OPT}} \right)} \cdot e^b \cdot e^{-\left(\frac{S_{INT} - S_{OPT}}{S_{OPT}} \right)}$	56	Cysteine governing equation $\frac{dCYS_{INT}}{dt} = A_{CYS:C} - CYS_{Mwas} - T_{CYS:C} - CYS_{INT} \cdot G$
Lotka-Volterra model equations			
57	Prey biomass governing equation $\frac{dPREY}{dt} = r \cdot PREY \cdot \left(1 - \frac{PREY}{K} \right) - PRED \cdot graz$		
58	Predator biomass governing equation $\frac{dPRED}{dt} = G \cdot PRED - m \cdot PRED - F \left(\frac{PRED^2}{PRED^2 + hz^2} \right)$		
59	Realized grazing rate $graz = gTz \cdot \left(\frac{PREY}{PREY + hz} \right)$		

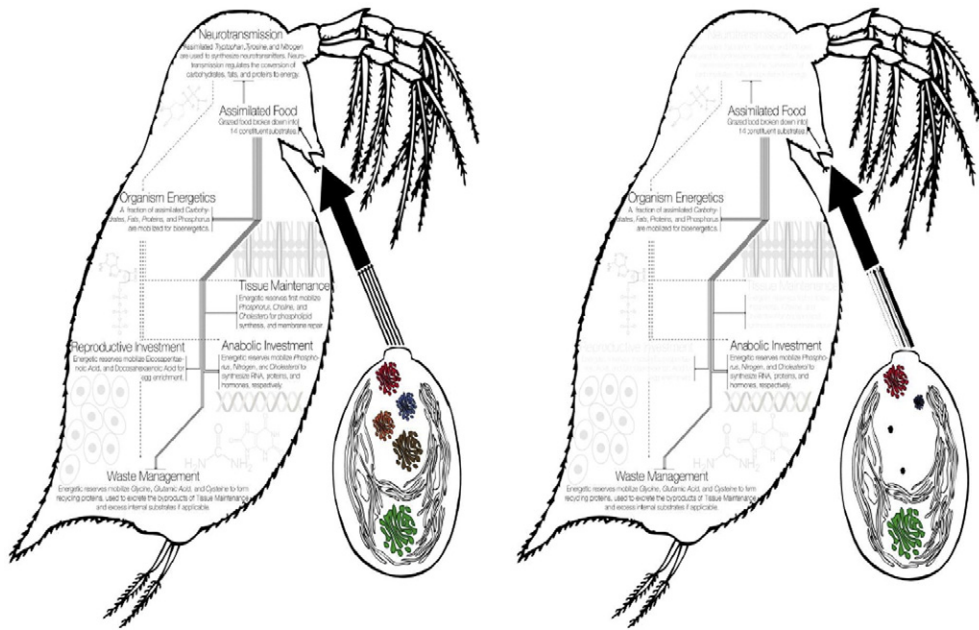


Fig. 2. Conceptual diagrams illustrating the transfer of congeners from algae to *Daphnia*, and the corresponding physiological ramifications.

physiological processes. A fraction of phosphorus is allocated to bio-energetics, and is used as a proxy for the ATP cycle. The neurologically-driven bottleneck of the energetic capacity is multiplied by both phosphorus saturation and the fraction allocated to bio-energetics to yield the final energetic capacity. Unutilized energetic compounds are assumed to be stored in their originating forms (e.g., carbohydrate, protein, and fat stores). At this point, the organism has two broadly categorized currencies: mass (ingested congeners expressed in congener:carbon ratios), and energy (expressed in Joules), and for the remaining physiological processes (i.e., downstream processes), there is a delicate interplay between the two currencies. Energetic allocation between the remaining processes is parameterized, and can be shaped to reflect various evolutionary and developmental goals. In this way, two differently parameterized individuals can experience vastly different dynamics in an identical environment. This also allows for our eco-physiological model to incorporate aspects of niche theory (Schoener, 2009), whereby differently parameterized individuals are selected for unique environments (see Fig. 2).

Our so-called downstream processes include osmoregulatory and tissue maintenance, removal of maintenance byproducts, homeostatic regulation (as required), and growth investments (somatic and reproductive). The aforementioned energetic fractionations determine how much of the energetic capacity is allocated to each process. This energetic value is then used to mobilize each of the congeners required in the physiological process. We assume maintenance processes are controlled by four congeners: fractions of dietary fat and phosphorus (for phospholipid formation), a fraction of cholesterol (CLS; for lipid raft

formation see Perhar et al., 2012), and choline (CHO; a phospholipid precursor). As a first approximation, we assume energy is equally distributed among the four maintenance congeners. Having quantified how much energy is acting upon each congener, we convert this measure into mass. These mass measures reflect how much ingested congener is utilized across the animal's body, and how much is added to the existing internal reserve. If energetic allocations call for more mass, then the organism digs into its internal reserves. This can only continue for a limited time, however, as saturation values can fall to zero, at which point the organism can no longer survive.

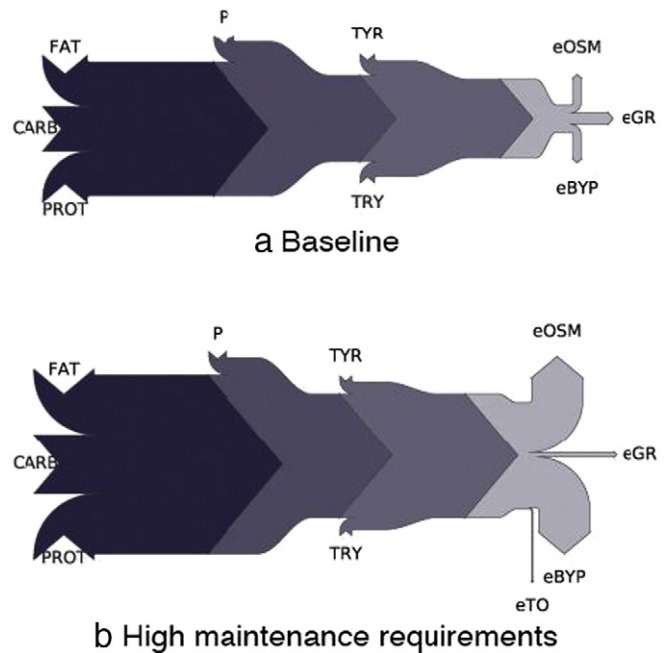


Fig. 3. Sankey diagrams illustrating the flow of energy in the modelled daphnid. Energetic flux is illustrated via arrow width. Potential energy is derived from ingested fuel congeners (i.e., FAT, CARB, PROT), and is subject to P- and neuro-limitations. The organism uses remaining energy (i.e., energetic capacity) to drive physiological processes.

Table 3
Lotka-Volterra model parameters, values, and units. Equation numbers refer to equations listed in Table 2.

Symbol	Description	Value	Unit	Equation
<i>grz</i>	Maximum zooplankton grazing rate	1.25	day ⁻¹	59
<i>K</i>	Algal carrying capacity	10	mg CL ⁻¹	57
<i>r</i>	Algal growth rate	0.85	day ⁻¹	57
<i>ha</i>	Algal grazing half saturation constant	5	mg CL ⁻¹	59
<i>hz</i>	Zooplankton grazing half saturation constant	2	mg CL ⁻¹	58
<i>F</i>	Fish predation rate	0.2	day ⁻¹	58
<i>m</i>	Zooplankton mortality rate	0.01	day ⁻¹	58
<i>G_{max}</i>	Maximum zooplankton growth rate	0.64	day ⁻¹	42

We assume a 1:1 ratio of byproduct removal, whereby the organism allocates identical reserves of energy to both maintenance and maintenance-related byproduct removal. We have assumed that the energy allocated to byproduct removal acts upon three mono-fated amino-acid congeners: cysteine (CYS), glycine (GLY), and glutamic acid (GA). These amino-acids are precursors to glutathione, a molecule strongly associated with detoxification in aquatic crustaceans (Billiard et al., 2008). Again, we assume an equal sub-fractionation between the three congeners. Next, we have hypothesized that the organism conducts a *sanity check* before it can invest resources into somatic and reproductive growth. Namely, it checks to see how far (if at all) it has deviated from homeostasis. We have quantified this as follows: if a subset of congeners is supersaturated (i.e., have internal concentrations greater than their respective optimal values), the organism has deviated from homeostasis. This can happen for a number of reasons, but is most likely related to an unbalanced diet, or a consequence of upstream forcing. If there is deviation from homeostasis, a fraction of remaining energy (destined for growth investment under ideal conditions) is used to turnover supersaturated congeners. This newly allocated energy is distributed among supersaturated congeners. While it is plausible that organisms excrete excess materials with bias, in the absence of such data, we have assumed an equal distribution. For example, if there are three supersaturated pools, one third of the regulatory-turnover energy is applied to each. While this is meant as a corrective-measure, we

hypothesize that this decision - under extreme circumstances - can turn into a run-away positive feedback cycle. Take for example, a situation where the organism is forced to divert growth energy in an attempt to regain homeostasis. This strategy results in a lower net growth investment, and a lower overall growth rate (see following section). This in turn is expected to mobilize smaller fractions of congeners, further adding to the issue of excessive congener accrual. We have modelled the turnover of excess matter using a sigmoidal relationship (Gompertz equation), whereby slow release rates are triggered with low supersaturation levels, followed by a rapid (approximately linear) turnover increase until a maximum release rate is established, when conditions of excessive congener accumulation prevail.

Energy remaining after maintenance, byproduct removal, and homeostatic adjustments (when necessary) is divided between somatic and reproductive growth investments. This delineation separates individuals with large developmental requirements from those with large reproductive drives. It can be argued that this delineation will shift with maturity: juveniles and non-sexually mature individuals will focus all of their energy on somatic growth, while mature individuals will have to consider both. Explicit daphnid development and maturation along with the associated priority shifts between anabolic growth and reproduction is outside the scope of the current study. Within the model, we have specifically allocated energy for somatic growth investment to act on fractions of cholesterol (reflecting production of growth

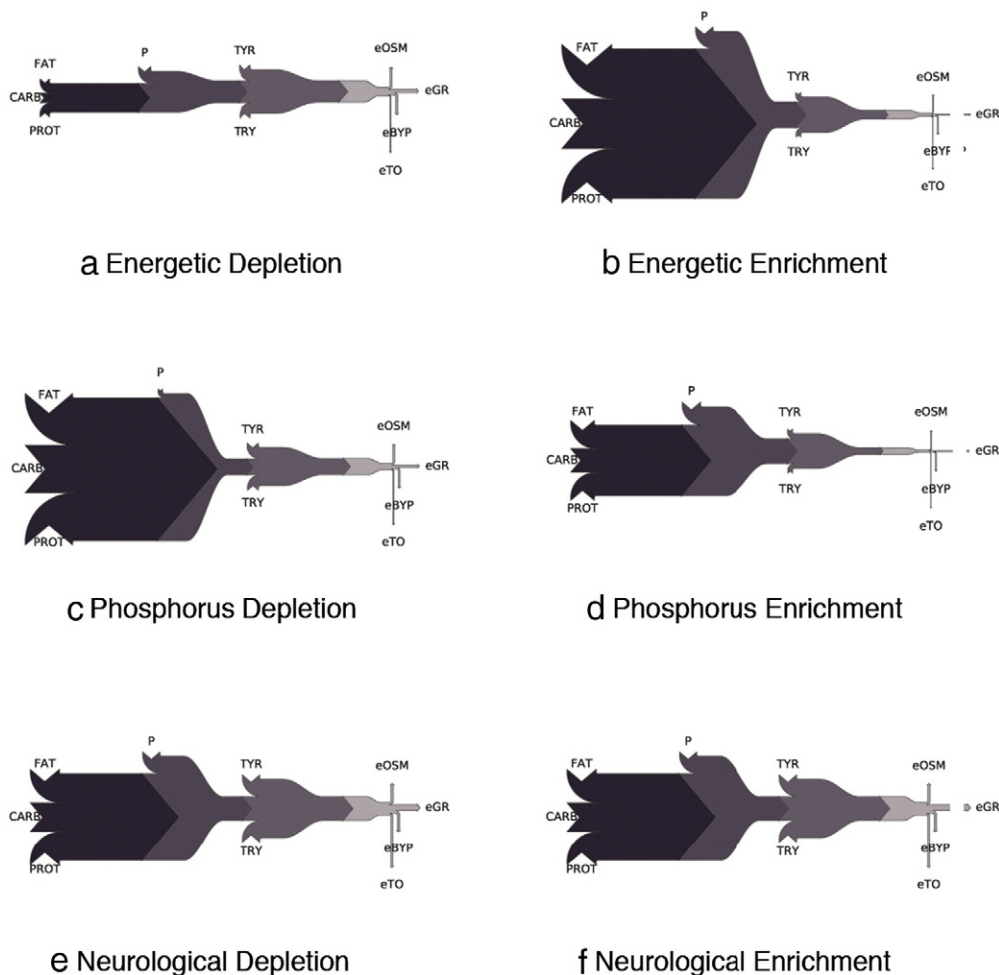


Fig. 4. Sankey diagrams illustrating the flow of energy in the modelled daphnid. Somatic energetic fluxes in response to variations in dietary energetic, phosphorus, neurological, reproductive, anabolic growth, and waste management congeners. Daphnid strategy was held constant at baseline conditions, and the affected algal congener concentrations were varied equally (i.e., 10% of baseline for low, 500% of baseline for high). Scenarios involving multiple congeners were varied equally, whereby each algal congener concentration was lowered to 10% or raised to 500%.

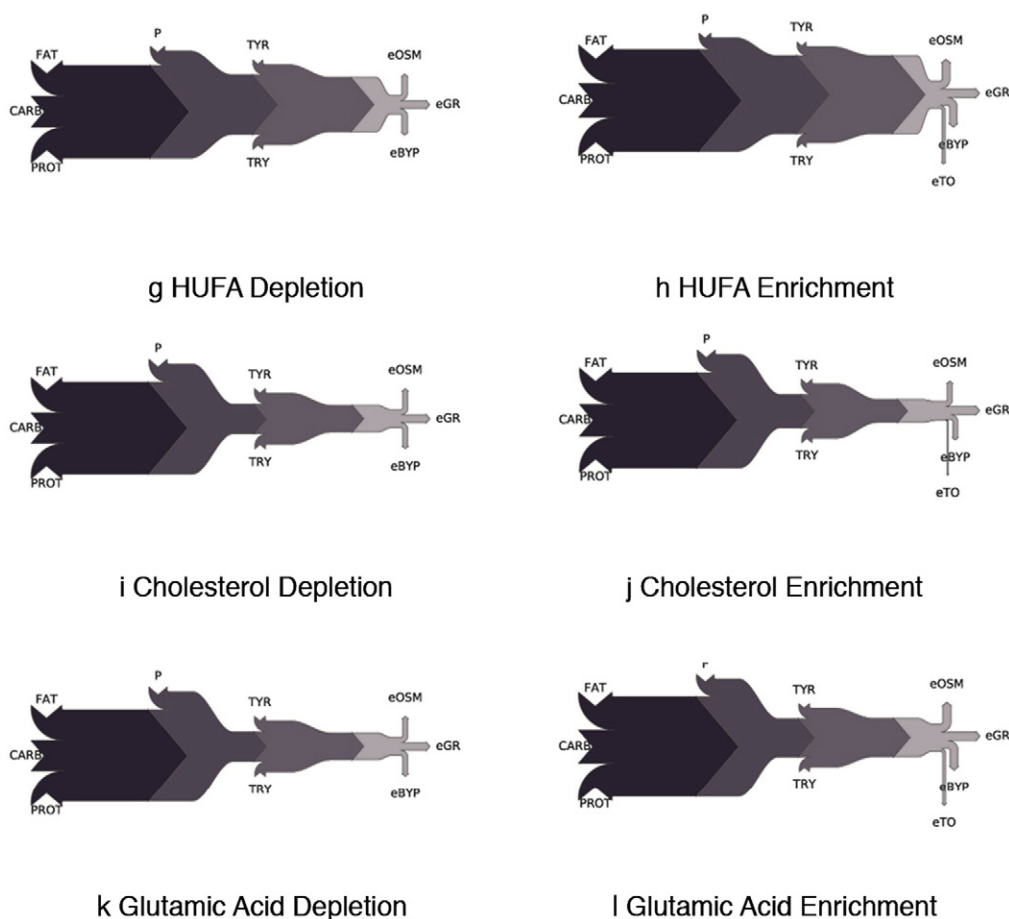


Fig. 4 (continued).

Table 4

Daily energetic signatures from grazing to growth. Listed entries include: potential energy (*POTENTIAL*), energy remaining post-ATP bottleneck (*BN1*), energy remaining post-neurological bottleneck (*BN2*), energy used for congener turnover (*TURNOVER*), and energy used for growth investments (*GROWTH*). HUFA = highly unsaturated fatty acids. Asterisks indicate scenarios that do not experience a neurological bottleneck.

Scenario	Units	POTENTIAL	BN1	BN2	TURNOVER	GROWTH
Baseline	J mg C ⁻¹	10.07	3.24	2.94	0	0.43
	%	100.0	32.2	29.2	0	4.2
Higher maintenance	J mg C ⁻¹	14.95	10.37	10.37*	0.05	0.19
	%	100.0	69.3	69.3	0.4	1.3
Energetic depletion	J mg C ⁻¹	1.54	1.16	1.16*	0.06	0.18
	%	100.0	75.7	75.7	3.8	11.4
Energetic enrichment	J mg C ⁻¹	21.36	1.48	0.50	0.02	0.05
	%	100.0	6.91	2.3	0.1	0.2
Phosphorus depletion	J mg C ⁻¹	15.94	0.89	0.89*	0.05	0.14
	%	100.0	5.6	5.6	0.3	0.9
Phosphorus enrichment	J mg C ⁻¹	3.85	1.36	0.38	0.01	0.04
	%	100.0	35.4	10.0	0.4	1.1
Neurologic depletion	J mg C ⁻¹	26.45	15.26	2.56	0.10	0.29
	%	100.0	57.7	9.7	0.4	1.1
Neurologic enrichment	J mg C ⁻¹	5.01	1.37	1.37*	0.11	0.34
	%	100.0	27.3	27.3	2.3	6.8
HUFA depletion	J mg C ⁻¹	10.07	3.24	2.94	0	0.43
	%	100.0	32.2	29.2	0	4.2
HUFA enrichment	J mg C ⁻¹	11.31	4.32	4.32*	0.16	0.49
	%	100.0	38.2	38.2	1.4	4.3
Cholesterol depletion	J mg C ⁻¹	10.07	3.24	2.94	0	0.43
	%	100.0	32.2	29.2	0	4.2
Cholesterol enrichment	J mg C ⁻¹	10.61	3.68	3.54	0.05	0.46
	%	100.0	34.6	33.3	0.5	4.3
Glutamic acid depletion	J mg C ⁻¹	10.07	3.24	2.94*	0	0.43
	%	100.0	32.2	29.2	0	4.2
Glutamic acid enrichment	J mg C ⁻¹	11.32	4.32	4.32*	0.16	0.49
	%	100.0	38.2	38.2	1.4	4.3

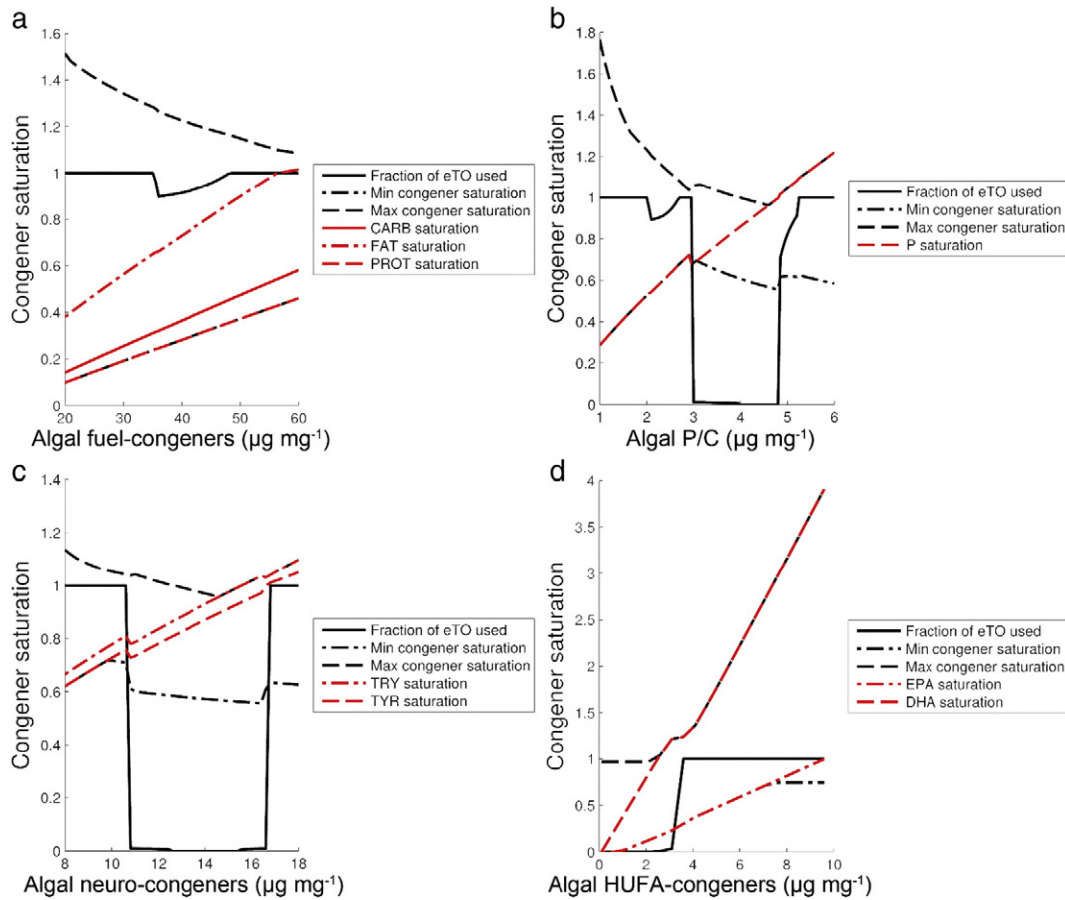


Fig. 5. Fraction of energy allocated to regulatory turnover (thick black line) used versus a) fuel congener enrichment, b) phosphorus enrichment, c) neuro-congener enrichment, d) HUFA enrichment. Saturations of enrichment congeners are shown in colour. The least and most saturated pools among the 14 congeners considered are shown in black dashed and dotted lines, respectively.

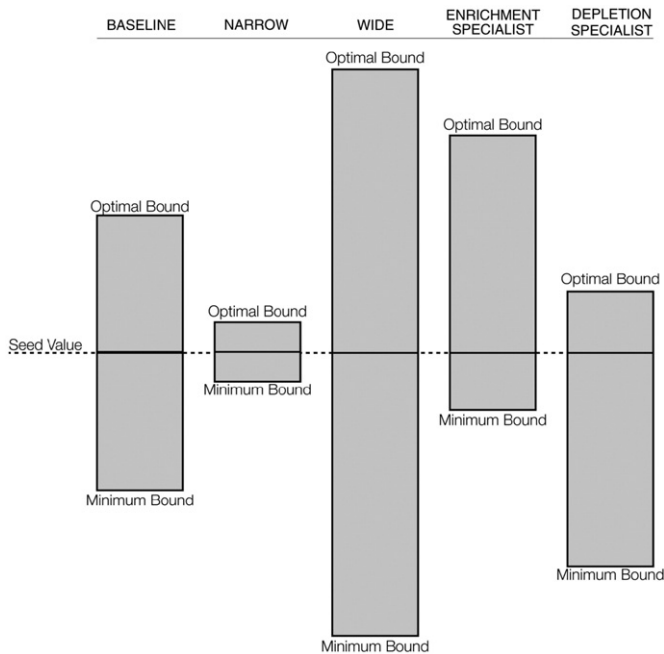


Fig. 6. Homeostatic classification scheme using a congener seed value around which upper and lower somatic congener bounds are formed. Using this scheme, individuals can be designated as narrow (very low optimum and very high minimum bounds), accommodating or wide (very high optimum and very low minimum bounds), optimized for depletion (very low minimum bound), or optimized for enrichment (very high optimum bound).

hormones and steroids; Heffner and Schust, 2010), and nitrogen and phosphorus (to represent their roles in nucleic acid synthesis; Alberts et al., 2002). Finally, we allocated energy for reproductive growth to act on two mono-fated congeners: eicosapentaenoic acid (EPA) and docosahexaenoic acid (DHA), to reflect their concentration in daphnid eggs, and their roles in sex hormone production (see Perhar et al., 2012). Daphnid growth rate is a fraction of its maximum parameterized growth rate. This fraction considers the amount of daily energy flux remaining for growth investment processes relative to the energetic use efficiency of our zooplankter, as specified by a new parameter (Ehs ; see Table S1) conceptually similar to the half-saturation constants typically used to depict the kinetics of enzymatic reactions.

The Lotka-Volterra predator-prey model consists of two differential equations, one for algae (prey) and one for *Daphnia* (predator), based on formulations presented by Scheffer et al. (2000). The predator population depends on the growth rate (G) of *Daphnia*, determined by the metabolite-driven sub-model described above, multiplied by the available predator biomass, minus losses from mortality and fish predation. Natural mortality rate, m , is fixed, while a type-III functional response was postulated to account for fish predation, characterized by a maximum fish predation rate, F , and a half-saturation value, hz . The algal population follows a classical logistic function with a maximum growth rate r , and carrying-capacity K . Losses due to zooplankton grazing follow a type-II functional response of algal biomass with an algal grazing half-saturation constant, ha , and a maximum zooplankton grazing rate, grz . Equations and parameters for the food-web component of the model are summarized in Tables 2 and 3, respectively.

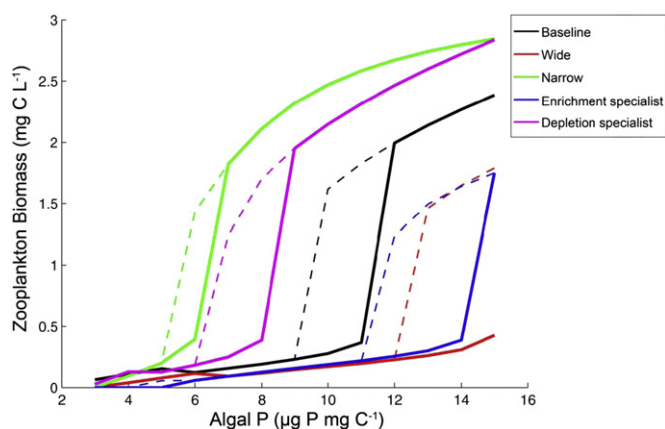


Fig. 7. Various homeostatic strategists in response to algal phosphorus enrichment (solid lines), and depletion (dashed lines). In each case, the system experiences hysteresis, whereby enrichment and depletion follow different trajectories.

3. Results-discussion

Energetic flow through the modelled daphnid is presented in a series of flow diagrams (see Figs. 3, 4). The energetic yield of fuel compounds (internal FAT, CARB, and PROT) is summed to form the organism's daily maximum potential energy. This potential energy is subject to a bottleneck if phosphorus saturation is <1 . This step is representative of the ATP cycle, and can modulate the individual's capacity to capitalize upon the existing energetic potential. Energetics are further subject to a neurological bottleneck if tryptophan or tyrosine saturations are below 1. This process is representative of nervous-system stress (e.g., limited neurotransmission), and like the previous bottleneck, controls the actual utilization of the daily energetic potential. The energy remaining after this second bottleneck is the organism's energetic capacity, and is used to drive maintenance, recycling, regulatory turnover, anabolic investment, and reproductive investment. Under our baseline scenario (Table 4; Fig. 3a), P saturation is approximately 97.5%. Thus, after accounting for the fraction of phosphorus allocated to energetics (33%), the energetic potential of consumed fat, carbohydrates, and protein is subject to an approximate 68% reduction and this is illustrated by arrow weights in the flow diagram: the flux into the phosphorus-bottleneck is larger than the flux out (or $10.07 \text{ J mg C}^{-1} \times 0.975 \times 0.33 = 3.24 \text{ J mg C}^{-1}$). Neurologic congeners tryptophan and tyrosine also have saturations below 1 (90.7% and 94%, respectively), and thus pose a minimal restriction to the utilization of the energetic potential (or $3.24 \text{ J mg C}^{-1} \times 0.907 = 2.94 \text{ J mg C}^{-1}$). Once past the neurological bottleneck, the remaining energy is used to drive physiological processes. Our baseline individual allocates 10% of its energetic capacity to maintenance (eOSM), which necessitates an additional 10% for recycling of maintenance byproducts (eBYP); see Eq. 32 in Table 2. The energetic remainder is put toward growth (eGR), encompassing both anabolic and reproductive investments. This example illustrates a well-balanced and optimally functioning individual, where congener availability in the food is being used efficiently. In particular, the individual is able to maintain all congener pools below the point of saturation, allowing for growth maximization. This in turn feeds back in the form of congener mobilization, further preventing unhealthy congener accumulation. In terms of the macroscopic patterns, the baseline scenario is characterized by a prey-to-predator ratio equal to one (Fig. S1). Under identical conditions, an individual with a physiological strategy out of synchronization with environmental conditions may not fare as well. Repeating the experiment with an individual highly focused on maintenance (45% of energetic capacity allotted to maintenance) yielded significantly different results (Table 4, Fig. 3b). While initial environmental conditions (i.e., food availability and congener concentrations) were identical, the organism exhibited markedly

different physiological energetic fluxes. Because this strategist allocates more resources to maintenance (as illustrated by the thicker flows to eOSM and eBYP), few resources remained for growth investment. This animal growth limitation led to a chain reaction, whereby resource mobilization rates slowed, and the majority of congener pools reached supersaturation. This supersaturation triggered the need for regulatory turnover (eTO), which further limited growth, and resulted in additional internal congener accumulation. Thus, even under seemingly ideal dietary conditions (e.g., energetic, neurological, and phosphorus supersaturation; Fig. 3b), a physiological strategy at the individual level that opts for higher energetic investment on maintenance can yield drastically different prey-predator dynamics relative to the baseline scenario (Fig. S1).

The mismatch between organismal strategies and environmental conditions can be a significant driver of ecological dynamics (Sternler and Elser, 2002). Thus, we investigated multiple aspects of food quality to gauge organism response. Specifically, we introduced variability in calorie-carrying (Fig. 4a, b), phosphorus (Fig. 4c, d), neurological (Fig. 4e, f), reproductive (Fig. 4g, h), anabolic growth (Fig. 4i, j), and waste management (Fig. 4k, l) congeners. Congener availability in algae was increased to 500% over the baseline scenario to mimic enrichment

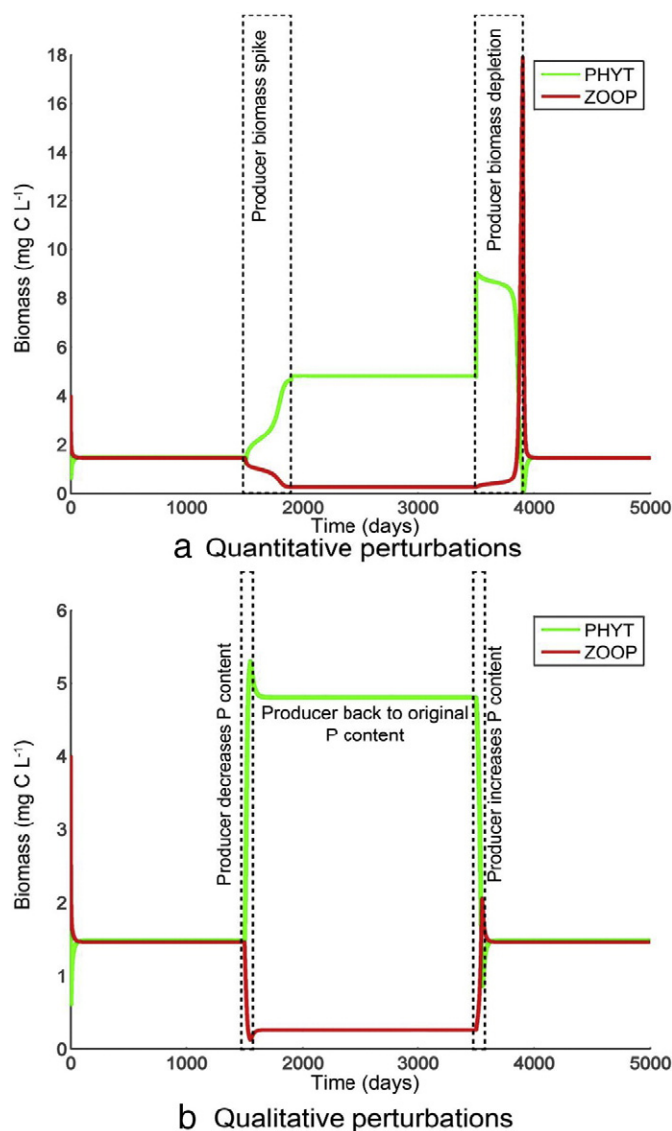


Fig. 8. Time series illustrating the effects of quantitative (i.e., biomass; a), and qualitative (i.e., congener availability; b) perturbations on food web equilibrium when characterized with a baseline daphnid.

conditions, and then reduced to 10% to reproduce resource limiting scenarios. The implications of the twelve scenarios are evaluated against the baseline individual portrayed in Fig. 3a. Organism response was visualized using energetic flow diagrams, in order to illustrate the effects of bottlenecks. When subject to energetic depletion, the lack of energetic potential was propagated through to low growth relative to the baseline scenario (Table 4, Fig. 4a). A direct effect of low realized growth is the lower congener mobilization rate, resulting in accumulation and (a seemingly paradoxical) supersaturation. In this case, supersaturation was experienced across many congener pools, necessitating regulatory turnover. From a macroscopic standpoint, the scenario of exposure to an energetically depleted diet is the least desirable, whereby high primary producer biomass coexists with low production at the higher trophic levels (Fig. S1; see also Brett and Muller-Navarra, 1997). When fuel congeners were available in abundance (i.e. energetic enrichment; Fig. 4b), our model predicts that the excessively high initial daily energetic capacity leads to the establishment of a steady state reflective of an inverted food web pyramid, where relatively low phytoplankton can sustain high zooplankton (and subsequently fish) biomass (Fig. S1). At the organismal level, this scenario suggests a high energetic potential that rapidly diminishes due to post-ATP and post-neurological bottlenecks imposed by severe phosphorus, and tryptophan/tyrosine limitations (Table 4; Fig. 4b), which in turn are predominantly driven by the algal food shortage. Notably, only a minor fraction of the energy capacity is utilized for regulatory turnover due to the supersaturated fuel congener concentrations.

Investigating the two potential bottlenecks yielded similar responses, whereby algal depletion of phosphorus (Fig. 4c), or tryptophan and tyrosine (Fig. 4e), resulted in large amounts of unutilized energy within the daphnid (Table 4). In both cases, growth was low enough for congener accumulation to occur across multiple pools, thereby triggering regulatory turnover. Phosphorus depletion had a more severe impact on daphnid growth rate than neurological congener depletion (Table 4, Fig. 4c, e), which likely reflects the broader implications of multi- versus mono-fated congeners. That is, while ingested phosphorus is used for energetics, maintenance, and anabolic investment, tryptophan and tyrosine are only used for neurotransmission. Thus, it is reasonable to assume the heightened sensitivity of growth on low phosphorus is due to this fractionation, whereby ingested phosphorus is reduced to 10% of reference conditions, but of the reduced intake, only a percentage is allocated to energetics. Similar reasoning can be applied to enrichment scenarios, where phosphorus-enrichment (Table 4, Fig. 4d) elicited an initially stronger growth response than neuro-enrichment (Table 4, Fig. 4f) leading to the establishment of a steady state with a six-fold predator-to-prey ratio (Fig. S1). In both cases, only the enriched pools achieved supersaturation, thereby triggering regulatory turnover; especially with the scenario of neurological enrichment.

The aspects of food quality considered to this point have been upstream, in the sense that they directly influence the energetic cycle. That is, fuel congeners define the maximum potential energy, which is then shaped by available phosphorus, tryptophan, and tyrosine, determining the individual's actual energetic capacity. This in turn regulates congener mobilization fractions and growth. Testing daphnid sensitivity to variations in algal HUFA, cholesterol, glutamic acid content, both the organism's response and the prey-predator patterns were nearly identical to baseline conditions (Table 4, Fig. 4g, i, k). The only difference was the extremely depleted pools of the corresponding congeners. By contrast, the examination of enrichment scenarios led to the establishment of a steady state with a prey-to-predator ratio < 1 (Fig. 4h, j, l), likely due to the supersaturation of the corresponding congeners that triggered regulatory turnover and thus lowered animal growth during the transient phase (Fig. S1). Interestingly, the higher algal food availability after the prey-predator system reaches its equilibrium phase results in both higher energetic potential and energetic investment (per unit of biomass) to growth under enrichment conditions.

In testing the effects of differential food quality stresses, the activation of regulatory turnover was a recurring pattern. That is, while fat, carbohydrate, protein, phosphorus, tryptophan, and tyrosine enrichment triggered regulatory turnover due to enrichment-related accumulation, so did depletion. This is indicative of a bottleneck phase, as illustrated by the Quadrant Metric in Perhar and Arhonditsis (2015) (see their Fig. 2). This behaviour was also apparent in the previous experiment's flow diagrams (Fig. 4), and was limited to upstream congeners. In contrast, EPA and DHA depletion did not trigger regulatory turnover, as there are no direct feedbacks to upstream congener dynamics. We compared congener saturations for the least and most saturated pools (across all 14 congeners), saturations of the enriched congeners under consideration, and the fraction of energy allocated to turnover being actively used (eTO; Fig. 5). In the current specification, our model sets the fraction of energy remaining after maintenance and byproduct removal for regulatory turnover to a maximum of 25%. That is, if the individual is straying from homeostasis, it can allocate up to one quarter of its growth energy towards regaining homeostatic balance. The fraction of energy mobilized to maintain homeostasis (eTO) illustrates the inherent hierarchy within the upstream congeners. An eTO = 0 indicates optimal daphnid functioning as a result of a balance diet. Three distinct patterns emerged under various algal (food) congener enrichment scenarios (Fig. 5). While phosphorus, tryptophan, and tyrosine enrichment passed through regions where all available energy was used for growth (i.e., eTO = 0; Fig. 5b, c), energy-related congeners did not pass through such a phase (Fig. 5a). There was a small decrease in the fraction of turnover energy used under energetic congener enrichment, but this fraction never dropped to 0% (Fig. 5a). Simply put, for a given algal content in non-fuel congeners (Table S2), our model conceptualization stipulates two scenarios with respect to the energetic content of the zooplankton diet that both result in non-zero regulatory turnover; namely, our zooplankton experiences (i) food items depleted in energy-related congeners, and therefore the lowered growth rate is accompanied by accumulation of non-fuel congeners which in turn triggers regulatory turnover; and (ii) energy-rich diets that plausibly accelerates turnover to discard the excess material. In addition, the eTO = 0 region only occurred when phosphorus or tyrosine (and for some portions tryptophan) were neither minimally nor maximally saturated (Fig. 5b, c). Under an algal HUFA enrichment scenario, regulatory turnover (eTO > 0) did not occur until DHA became supersaturated, while EPA was always minimally saturated (Fig. 5d). Taken together, these results suggest that there is an optimal algal congener composition that optimizes *Daphnia's* internal congener saturations, resulting in a maximal allocation of energy to growth. This optimal diet consists of mid-ranged phosphorus and neurological congener concentrations. The "stoichiometric knife edge" theory implies that optimal food contains a balanced nutrient content (Elser et al., 2012); recent stoichiometrically explicit algal-herbivore models have demonstrated that consumer growth is reduced by food with both too little, and too much, phosphorus content (Peace et al., 2013, 2014). Our model further extends this concept, demonstrating that not just stoichiometric nutrients, but multiple (e.g., neurological, fatty acid) congeners must also exist in balanced proportions in order for *Daphnia* to achieve optimal growth.

We define our daphnid's homeostatic bounds using literature-driven "seed" values for each congener. These "seed" values are then inflated and deflated to create optimum and minimum somatic resource bounds, respectively (Fig. 6). For example, if an individual's homeostatic range is defined by inflation and deflation factors of 1.25 and 0.75, respectively, the organism's somatic congener concentrations cannot fall below 75% of the seed values, and implies malnutrition-related stress if somatic congener concentrations are > 125% of the seed values. This characterization scheme is the second instance where the model allows to differentiate zooplankton behaviour based on physiological strategies (the first being energetic allocation between physiological processes). For example, if an individual has very low optimum, and very high minimum bounds, it will have a very narrow congener range in which the

animal can function optimally and therefore demonstrates rigid stoichiometric behaviour (*narrow strategist*; Fig. 6). Conversely, if an individual has a very high optimum bound combined with a very low minimum bound, it is characterized by a more dynamic stoichiometry and will be referred to as a *wide strategist*. We also considered specialized species with a similar quota range as the baseline individual, but with shifted optimal and minimal bounds, such that they thrive under enrichment (i.e., very high optimum bound; *enrichment specialist*), or depletion (i.e., very low minimum bound; *depletion specialist*) conditions (Fig. 6). Organisms with very narrow homeostatic bounds are expected to perform poorly against wide strategists in volatile environments with respect to the quantity and quality of their diet, experiencing both somatic resource limitation and supersaturation quicker than their counterparts. If conditions are within their nutritional requirements, however, narrow strategists can outperform wide strategists because with all else being equal, they will tend to have higher somatic saturations, which would alleviate bottlenecks, resource mobilizations, and eventually growth. A wide strategist, on the other hand, will opt for a “slow burn” strategy, displaying more muted responses to external fluctuations.

In a phosphorus-enrichment scenario relative to the default food quality conditions (Table S2), organisms with narrow homeostatic bounds achieve optimal performance first (Fig. 7). The next specification to reach optimal performance is the depletion specialist. In addition, both the narrow strategist and depletion specialist achieve a higher biomass at lower algal phosphorus concentrations than the baseline individual (Fig. 7). In contrast, the enrichment and wide strategists are the last to achieve optimal functioning, respectively. [It is important to note that our exercise does not consider the likelihood of covariance between somatic quotas and physiological rates, which can further modulate the response of the individual zooplankters to algal food quality variations.] When repeating the same experiment in reverse (i.e., phosphorus depletion), we found regions where enrichment and depletion trajectories (Fig. 7, solid and dashed lines, respectively) did not coincide. These patterns are indicative of multiple stable equilibria in the Lotka-Volterra system (sensu Scheffer et al., 2001), and the ranges of multiple equilibria were proportional to a strategist's congener spread. That is, the narrower the daphnid homeostatic range, the smaller the range of algal phosphorus concentrations over which multiple equilibria occurred (Fig. 7). It is worth noting that congener spread alone does not dictate the system's tendency to spawn multiple attractors. Multiple steady state equilibria are plausible in different regions of phase space, when examining enrichment or depletion scenarios for different congeners, or altering the non-phosphorus congener values in the current experiment. Within the constraints of the current experiment, however, the magnitude of congener spread was an important factor in determining the system's likelihood to experience multiple attractors. Thus, modelling approaches not considering congener quotas (i.e., models with fixed stoichiometric requirements) would be expected to experience identical trajectory-dynamics across resource enrichment and depletion scenarios. In addition, depending on the specification of the organism, the system may be able to experience various equilibria states. For example, with algal phosphorus concentrations ranging from 5 to 6 $\mu\text{g P mg C}^{-1}$, systems with zooplankters of narrow nutrient quotas can be either in a state of low producer to consumer or high producer to consumer ratios. In the same scenario, if the same system were characterized by *Daphnia* of any other specification, there would be only one steady state equilibrium. In other words, systems with *Daphnia* of various characteristics will be prone to multiple attractors at different congener availabilities.

In the aforementioned regions where the system is prone to multiple equilibria endpoints, perturbations can conceivably shift the system from one equilibrium to another (Scheffer et al., 2001). Thus, if the conditions are right, and the perturbation is of an appropriate magnitude and duration, the system may not recover to its initial state. Studies have illustrated this dynamic in the context of quantitative imbalances,

whereby a large influx of biomass (or depletion of biomass) can irreversibly alter the food web's structure (see examples in Beck, 2013). In a similar manner, we were able to reproduce this pattern in our model by artificially inflating phytoplankton biomass (Fig. 8a). By incrementally increasing phytoplankton biomass for a certain amount of time, the system settled to an alternate equilibrium characterized by a high producer to consumer biomass ratio. Once the system settled to this equilibrium, no artificial inflation of phytoplankton biomass was required to maintain this high producer-to-consumer ratio. We were able to switch back to the previous equilibrium by instantaneously removing a portion of the phytoplankton biomass. The system responded with increased zooplankton biomass, and a temporarily increasing phytoplankton biomass, but soon settled back to its initial equilibrium characterized by a producer-to-consumer ratio of approximately 1. More interestingly, we were also able to induce equilibria shifts from a qualitative standpoint (Fig. 8b). In this instance, we overrode phytoplankton's phosphorus content for a short period, restored normal conditions, then overrode phytoplankton phosphorus content again for a second short period before returning to normal conditions. The two spikes (i.e., the period starting at time step 1500, and the period starting at time step 3500) were enough to shift the system into alternate steady states. In the first spike, we altered phytoplankton to be less nutritious, through a lower phosphorus concentration. The ramifications of this were realized almost instantly, as zooplankton biomass fell sharply, which likely triggered the sharp rise in phytoplankton. Following the spike, phytoplankton phosphorus concentration was reset to pre-spike conditions, but producer and consumer biomass values did not return to their initial states. Rather, they held steady in their new equilibrium. In the second spike, we made phytoplankton more nutritious, through heightened phosphorus content. The ramifications of this were, again, realized almost immediately, as zooplankton biomass increased sharply and phytoplankton biomass fell. Following this second spike, the system settled to a pre-spike prey-to-predator ratio of 1, effectively illustrating the potential back and forth nature of a system with multiple steady states.

4. Concluding remarks-future perspectives

Representing a freshwater food web with a Lotka-Volterra model is admittedly a simplification. By incorporating *Daphnia*'s physiological dynamics into the model, we have effectively included a complex set of intra-organismal dynamics nested within the producer-consumer interactions. Specifically, homeostatic spread - or the difference between minimum viable congener concentration, and optimal congener concentration - assigns a buffer capacity to the consumer to cope with the variability of the food quantity and quality. For example, in the case of enrichment followed by depletion with a large homeostatic spread, the system exhibits very different dynamics along both trajectories. This macroscopic complexity is entirely due to the internal processing of *Daphnia*. Along an enrichment trajectory, zooplankton biomass jumps to a higher standing biomass once a critical physiological point has been reached. In our analysis, we found that this critical physiological threshold is consistent across all strategists and all environmental conditions. Similarly, along a depletion trajectory, the system settles to an alternate equilibrium characterized by a shift in zooplankton biomass to a significantly lower state once a critical physiological point has been reached. This response will not emerge in models not accounting for organismal nutritional and energetic variability.

This “outside in-inside out effect, with a physiological buffer in between” draws parallels with cybernetics, a branch of science detailing the goal-seeking aspect of system behaviour (Wiener, 1947). Stemming from the Greek word for art of steering, cybernetics can be summarized as the science of feedback, information, and goals (Ramkrishna and Song, 2012). As it stands now, our modelled daphnid is not an explicit cybernetic organism. While it uses feedback and system information to determine its performance, it does not dynamically adjust its

behaviour based on environmental feedback. This is a likely next step, whereby we would build on the existing definition of organism strategy. Currently, organism strategies are defined with energetic partitioning, and homeostatic spread. A likely third dimension to this would be the extent to which energetic partitioning could be adjusted. For example, the most flexible strategist could be defined with a large homeostatic spread, and a very dynamic energetic partitioning scheme. Conversely, a more conservative strategist would be one with a narrow spread, and a very limited ability to adjust its energetic scheme. To our knowledge, this is an aspect of model parameterization that has not been explored (i.e., the time explicit automatic logic-driven adjustment of parameters) that will unleash a new level of detail, with the potential for a closer-to-nature approximation in the current generation of food-web models.

We have presented a first-generation approximation of *Daphnia* physiology, and as such have made several simplifications in the name of pragmatism. One simplification is the role of each congener in the animal's physiology. We have considered several classes of congeners (e.g., mineral nutrients, fatty acids, amino acids, neurotransmitter proxies, waste management proxies, energetic congeners, and various other building blocks), and associated them with various aspects of *Daphnia* physiology. Some congeners are mono-fated, while others have multiple fates. This issue likely needs to be addressed, as most congeners should not only be substitutable (to an extent) with other congeners, but also be expected to play multiple roles within the body. Arguably, the most dynamic congener in our system is phosphorus. It is actively used in bioenergetics, maintenance, and somatic growth investment within the animal's body. Previous studies of *Daphnia* justified the use of phosphorus as the primary limiting reagent due to its role in RNA replication (Elser et al., 2003). In the context of our study, we assumed that phosphorus' most important facet is its role in bioenergetics (i.e., reflecting dynamics of the ATP cycle). We observed our model to switch from one steady state equilibrium to another once certain energetic capacity critical points were reached. Similar tipping points were not observed in maintenance, nor somatic growth investment modules. This could also be the underlying cause of phosphorus' sensitivity under depletion conditions, as its depletion is felt across multiple modules within the organism's hierarchical framework. Coincidentally, many downstream congeners are mono-fated. Fatty acids EPA and DHA are used only for reproductive investment, while amino acids cysteine, glycine, and glutamic acid are only used in waste management. These congeners are consistently the least impactful on organism functioning, as their depletion does not adversely affect upstream processes. If, however, there were links to upstream processes via a neurological feedback in the case of DHA, and restorative force dynamics in the case of the aforementioned amino acids, our daphnid would not only be a more closed system with tighter feedbacks, but also more closely resemble reality.

Highly complex ecological systems require a wide range of modelling approaches in order to understand their emergence and functioning (DeAngelis and Grimm, 2014). The Lotka-Volterra equations were a breakthrough in dynamic modelling a century ago when they were first developed, yet are admittedly simplifications of complex interactions among predators and their prey. Coupling our daphnid sub-model to a Lotka-Volterra food web model was a strategic choice, to gain a first approximation of food web level effects due to varying consumer internal physiology. Consequently, our results may be a reflection of this simplification. For example, we have observed multiple internal conditions that can yield identical food web level conditions. Similarly, large-scale changes in internal conditions can make little to no impact on macroscopic food web dynamics in some instances, while in others the slightest internal shift can cause dramatic shifts at the macroscale. In this sense, the model is exhibiting weak emergence, whereby various combinations of the model's subcomponents come together to form macroscopic patterns. In contrast to the Lotka-Volterra family of models, which are based on differential equations where the outcomes are predestined by assumptions made in those equations,

agent-based models (whereby individual daphnids are modelled instead of overall biomass) are increasingly acknowledged to provide more realistic answers to fundamental food web questions (Railsback and Grimm, 2011). Our current approach utilizes a lumped population-level model that assumes average properties of a population (Hellweger and Kianirad, 2007). By allowing consumers to behave realistically, through the addition of goal-seeking behaviour, such that individuals undertake actions based on choices that maximize their goal (i.e., increase individual fitness), stronger emergence patterns will likely be attainable (DeAngelis and Grimm, 2014). Moving towards an agent-based platform also has the advantage of a microscopic to macroscopic perspective, to explore how variations in internal physiology influence individual decisions (to maximize fitness), and ultimately food web properties, under varying environmental conditions. Further, an agent-based setting would enable us to examine variations across the life-cycle of our daphnid, as well as explore the interplay of HUFA congeners on energetic partitioning between reproduction and somatic growth. Once variability is introduced at the agent-level (i.e., strategies, requirements, and behaviours are resolved to the individual level instead of the population level as presented here), we will undoubtedly gain further insight into food web dynamics.

Perhar and Arhonditsis (2015) used the ecophysiology (sub)model to demonstrate that the energetic requirements of homeostasis can compromise daphnid growth under an imbalanced diet. By coupling the Perhar and Arhonditsis (2015) growth sub-model to a Lotka-Volterra predator-prey model, we have demonstrated the consequences of this variability in *Daphnia* internal physiological processes on food web dynamics: variations in homeostatic strategies and dietary conditions resulted in variations in energetic partitioning allocated for daphnid growth, which was manifested in alternative ecosystem states, characterized by dramatically different algal and zooplankton standing stocks (i.e., biomass). The high energetic costs to maintain homeostasis when *Daphnia* consumes an imbalanced diet occurred for multiple congeners, not just macronutrients (i.e., phosphorus); although supersaturation of multi-fated congeners (e.g. phosphorus, neurological) had a larger impact on energetic partitioning than mono-fated ones (e.g., HUFAs). Further, dietary daphnid enrichment and depletion trajectories induced hysteresis effects at the population level (i.e., in zooplankton biomass). Moving beyond the simplicity of Lotka-Volterra models, to an agent-based platform, will require a shift towards a microscopic perspective (i.e. characterizing internal *Daphnia* physiology). In future, working tightly with metabolomics data will provide a way forward for a more accurate portrayal of the combined responses of multiple metabolites to dietary variation or environmental stressors (e.g., Wagner et al., 2015), revolutionize our understanding of *Daphnia* physiology, and ultimately algal-grazer dynamics, in aquatic ecosystems.

Acknowledgments

This project has received funding support from the Krembil Foundation. Additional funding for Gurbir Perhar was provided by a MITACS Ellevate Postdoctoral Fellowship.

References

- Alberts, B., Johnson, A., Lewis, J., Raff, M., Roberts, K., Walter, P., 2002. DNA Replication, Repair, and Recombination. fourth ed. *Molecular Biology of the Cell*. Garland Science, New York, USA.
- Altschuler, I., Demiri, B., Xu, S., Constantin, A., Yan, N.D., Cristescu, M.E., 2011. An integrated multi-disciplinary approach for studying multiple stressors in freshwater ecosystems: *Daphnia* as a model organism. *Integr. Comp. Biol.* 51, 623–633. <http://dx.doi.org/10.1093/icb/icr103>.
- Andersen, T., 1997. Grazers as Sources and Sinks for Nutrients: Conclusions, Limitations, and Speculations, in: *Pelagic Nutrient Cycles Herbivores as Sources and Sinks*. Springer, Berlin Heidelberg, pp. 207–213 http://dx.doi.org/10.1007/978-3-662-03418-7_7.
- Andersen, T., Elser, J.J., Hessen, D.O., 2004. Stoichiometry and population dynamics. *Ecol. Lett.* 7, 884–900. <http://dx.doi.org/10.1111/j.1461-0248.2004.00646.x>.

- Anderson, T.R., Hessen, D.O., Elser, J.J., Urabe, J., 2005. Metabolic stoichiometry and the fate of excess carbon and nutrients in consumers. *Am. Nat.* 165, 1–15.
- Arhonditsis, G.B., Brett, M.T., 2005a. Eutrophication model for Lake Washington (USA). Part I. Model description and sensitivity analysis. *Ecol. Model.* 187 (2–3), 140–178. <http://dx.doi.org/10.1016/j.ecolmodel.2005.01.040>.
- Arhonditsis, G.B., Brett, M.T., 2005b. Eutrophication model for Lake Washington (USA). Part II. Model calibration and system dynamics analysis. *Ecol. Model.* 187 (2–3), 179–200. <http://dx.doi.org/10.1016/j.ecolmodel.2005.01.039>.
- Beck, T., 2013. Principles of Ecological Landscape Design. Island Press, Washington, DC.
- Billiard, S.M., Meyer, J.N., Wassenberg, D.M., Hodson, P.V., Giulio, R.T.D., 2008. Non-additive effects of PAHs on early vertebrate development: mechanisms and implications for risk assessment. *Toxicol. Sci.* 105, 5–23.
- Brett, M.T., Muller-Navarra, D.C., 1997. The role of highly unsaturated fatty acids in aquatic food web processes. *Freshw. Biol.* 38, 483–499. <http://dx.doi.org/10.1046/j.1365-2427.1997.00220.x>.
- DeAngelis, D.L., Grimm, V., 2014. Individual-based models in ecology after four decades. *F1000Prime Rep.* 6 39 10.12703/P6-39.
- Droop, M., 1968. Vitamin B12 and marine ecology. IV. The kinetics of uptake, growth and inhibition in *Monochrysis lutheri*. *J. Mar. Biotechnol.* 48, 689–733.
- Elser, J.J., Goldman, C.R., 1991. Zooplankton effects on phytoplankton in lakes of contrasting trophic status. *Limnol. Oceanogr.* 36, 64–90. <http://dx.doi.org/10.4319/lo.1991.36.1.0064>.
- Elser, J.J., Urabe, J., 1999. The stoichiometry of consumer-driven nutrient recycling: theory, observations, and consequences. *Ecology* 80, 735–751.
- Elser, J.J., Acharya, K., Kyle, M., Cotner, J., Makino, W., Markow, T., Watts, T., Hobbie, S., Fagan, W., Schade, J., Hood, J., Sterner, R.W., 2003. Growth rate-stoichiometry couplings in diverse biota. *Ecol. Lett.* 6, 936–943.
- Elser, J.J., Loladze, I., Peace, A.L., Kuang, Y., 2012. Lotka re-loaded: modeling trophic interactions under stoichiometric constraints. *Ecol. Model.* 245, 3–11. <http://dx.doi.org/10.1016/j.ecolmodel.2012.02.006>.
- Grimm, V., 1999. Ten years of individual-based modelling in ecology: what have we learned and what could we learn in the future? *Ecol. Model.* 115, 129–148.
- Grimm, V., Berger, U., Bastiansen, F., Eliassen, S., Ginot, V., Giske, J., Goss-Custard, J., Grand, T., Heinz, S.K., Huse, G., Huth, A., Jepsen, J.U., Jørgensen, C., Mooij, W.M., Müller, B., Pe'er, G., Piuu, C., Railsback, S.F., Robbins, A.M., Robbins, M.M., Rossmanith, E., Rüter, N., Strand, E., Souissi, S., Stillman, R.A., Vabø, R., Visser, U., DeAngelis, D.L., 2006. A standard protocol for describing individual-based and agent-based models. *Ecol. Model.* 198, 115–126. <http://dx.doi.org/10.1016/j.ecolmodel.2006.04.023>.
- Grimm, V., Berger, U., DeAngelis, D.L., Polhill, J.G., Giske, J., Railsback, S.F., 2010. The ODD protocol: a review and first update. *Ecol. Model.* 221, 2760–2768. <http://dx.doi.org/10.1016/j.ecolmodel.2010.08.019>.
- Heffner, L.J., Schust, D.J., 2010. The Reproductive System at a Glance. third ed. John Wiley and Sons, Ltd., New York.
- Hellweger, F.L., Kianirad, E., 2007. Individual-based modeling of phytoplankton: evaluating approaches for applying the cell quota model. *J. Theor. Biol.* 249, 554–565.
- Huston, M., DeAngelis, D., Post, W., 1988. New computer models unify ecological theory. *Bioscience* 38, 682–691.
- Koide, Y., Yoshida, A., 1994. The signal transduction mechanism responsible for gamma interferon-induced indoleamine 2,3-dioxygenase gene expression. *Infect. Immun.* 62, 948–955.
- Kooijman, S.A.L.M., 2010. Dynamic Energy Budget Theory for Metabolic Organisation. third ed. Cambridge University Press, New York, USA.
- Kovacevic, V., Simpson, A.J., Simpson, M.J., 2016. ¹H NMR-based metabolomics of *Daphnia magna* responses after sub-lethal exposure to triclosan, carbamazepine and ibuprofen. *Comparative Biochemistry and Physiology Part D: Genomics and Proteomics* <http://dx.doi.org/10.1016/j.cbd.2016.01.004>.
- Lankadurai, B.P., Nagato, E.G., Simpson, M.J., 2013. Environmental metabolomics: an emerging approach to study organism responses to environmental stressors. *Environ. Rev.* 21, 180–205.
- Li, L., Wu, H., Ji, C., Gestel, C.A.M., van Allen, H.E., Peijnenburg, W.J.G.M., 2015. A metabolic study on the responses of *Daphnia magna* exposed to silver nitrate and coated silver nanoparticles. *Ecotoxicol. Environ. Saf.* 119, 66–73.
- Liebig, J., 1840. Die organische Chemie in ihrer Anwendung auf Agricultur und Physiologie (Organic Chemistry in its Applications to Agriculture and Physiology). Friedrich Vieweg und Sohn Publishing Company, Braunschweig, Germany.
- Loladze, I., Kuang, Y., Elser, J.J., 2000. Stoichiometry in producer-grazer systems: linking energy flow with element cycling. *Bull. Math. Biol.* 62, 1137–1162. <http://dx.doi.org/10.1006/bulm.2000.0201>.
- Martin, B.T., Zimmer, E.I., Grimm, V., Jager, T., 2012. Dynamic energy budget theory meets individual-based modelling: a generic and accessible implementation. *Methods Ecol. Evol.* 3, 445–449. <http://dx.doi.org/10.1111/j.2041-210X.2011.00168.x>.
- Martin, B.T., Jager, T., Nisbet, R.M., Preuss, T.G., Grimm, V., 2013a. Predicting population dynamics from the properties of individuals: a cross-level test of dynamic energy budget theory. *Am. Nat.* 181, 506–519. <http://dx.doi.org/10.1086/669904>.
- Martin, B.T., Jager, T., Nisbet, R.M., Preuss, T.G., Hammars-Wirtz, M., Grimm, V., 2013b. Extrapolating ecotoxicological effects from individuals to populations: a generic approach based on dynamic energy budget theory and individual-based modeling. *Ecotoxicology* 22, 574–583. <http://dx.doi.org/10.1007/s10646-013-1049-x>.
- McCauley, E., Murdoch, W.W., Nisbet, R.M., Gurney, W.S.C., 1990. The physiological ecology of *Daphnia*: development of a model of growth and reproduction. *Ecology* 71, 703–715.
- McCauley, E., Nisbet, R.M., de Roos, A.M., Murdoch, W.W., Gurney, W.S.C., 1996. Structured population models of herbivorous zooplankton. *Ecol. Monogr.* 66, 479–501.
- Mooij, W.M., Hülsmann, S., Vijverberg, J., Veer, A., Lammens, E.H.R.R., 2003. Modeling *Daphnia* population dynamics and demography under natural conditions. *Hydrobiologia* 491, 19–34 10.1023/A.
- Mulder, K., Bowden, W.B., 2007. Organismal stoichiometry and the adaptive advantage of variable nutrient use and production efficiency in *Daphnia*. *Ecol. Model.* 202, 427–440. <http://dx.doi.org/10.1016/j.ecolmodel.2006.11.007>.
- Muller, E.B., Nisbet, R.M., Kooijman, S.A.L.M., Elser, J.J., McCauley, E., 2001. Stoichiometric food quality and herbivore dynamics. *Ecol. Lett.* 4, 519–529.
- Nagato, E.G., D'eon, J.C., Lankadurai, B.P., Poirier, D.G., Reiner, E.J., Simpson, A.J., Simpson, M.J., 2013. Chemosphere H NMR-based metabolomics investigation of *Daphnia magna* responses to sub-lethal exposure to arsenic, copper and lithium. *Chemosphere* 93, 331–337. <http://dx.doi.org/10.1016/j.chemosphere.2013.04.085>.
- Nisbet, R.M., McCauley, E., Gurney, W.S.C., Murdoch, W.W., de Roos, A.M., 1997. Simple representations of biomass dynamics in structured populations. In: Othermer, H.G., Adler, F.R., Lewis, M.A., Dallon, J.C. (Eds.), Case Studies in Mathematical Modeling – Ecology, Physiology, and Cell Biology. Prentice-Hall, Inc., New Jersey, pp. 61–80 577/01/5118 21.
- Nisbet, R.M., Muller, E.B., Lika, K., Kooijman, S.A.L.M., 2000. From molecules to ecosystems through dynamic energy budget models. *J. Anim. Ecol.* 69, 913–926.
- Nisbet, R.M., McCauley, E., Johnson, L.R., 2010. Dynamic energy budget theory and population ecology: lessons from *Daphnia*. *Philos. Trans. R. Soc. B* 365, 3541–3552. <http://dx.doi.org/10.1098/rstb.2010.0167>.
- Paloheimo, J.E., Crabtree, S.J., Taylor, W.D., 1982. Growth model of *Daphnia*. *Can. J. Fish. Aquat. Sci.* 39, 598–606.
- Peace, A., Zhao, Y., Loladze, I., Elser, J.J., Kuang, Y., 2013. A Stoichiometric Producer-Grazer Model Incorporating the Effects of Excess Food-Nutrient Content on Consumer Dynamics. 244 pp. 107–115.
- Peace, A., Wang, H., Kuang, Y., 2014. Dynamics of a producer-grazer model incorporating the effects of excess food nutrient content on grazer's growth. *Bull. Math. Biol.* 76, 2175–2179. <http://dx.doi.org/10.1007/s11538-014-0006-z>.
- Peeters, F., Li, J., Straiile, D., Rothhaupt, K., Vijverberg, J., 2010. Influence of low and decreasing food levels on *Daphnia*–algal interactions: numerical experiments with a new dynamic energy budget model. *Ecol. Model.* 221, 2642–2655. <http://dx.doi.org/10.1016/j.ecolmodel.2010.08.006>.
- Perhar, G., Arhonditsis, G.B., 2012. Examination of the role of detritus food quality, phytoplankton intracellular storage capacity, and zooplankton stoichiometry on planktonic dynamics. *Ecol. Inform.* 11, 76–89. <http://dx.doi.org/10.1016/j.ecoinf.2012.06.002>.
- Perhar, G., Arhonditsis, G.B., 2015. Development of a metabolite-driven *Daphnia* ecophysiological model. *Ecol. Inform.* 30, 82–96. <http://dx.doi.org/10.1016/j.ecoinf.2015.09.002>.
- Perhar, G., Arhonditsis, G.B., Brett, M.T., 2012. Modelling the role of highly unsaturated fatty acids in planktonic food web processes: a mechanistic approach. *Environ. Rev.* 20, 155–172. <http://dx.doi.org/10.1139/a2012-007>.
- Perhar, G., Arhonditsis, G.B., Brett, M.T., 2013a. Modeling zooplankton growth in Lake Washington: a mechanistic approach to physiology in a eutrophication model. *Ecol. Model.* 258, 101–121.
- Perhar, G., Arhonditsis, G.B., Brett, M.T., 2013b. Modelling the role of highly unsaturated fatty acids in planktonic food web processes: sensitivity analysis and examination of contemporary hypotheses. *Ecol. Inform.* 13, 77–98. <http://dx.doi.org/10.1016/j.ecoinf.2012.10.005>.
- Poynton, H.C., Taylor, N.S., Hicks, J., Colson, K., Chan, S., Clark, C., Scanlan, L., Loguinov, A.V., Vulpe, C., Viant, M.R., 2011. Metabolomics of microliter hemolymph samples enables an improved understanding of the combined metabolic and transcriptional responses of *Daphnia magna* to cadmium. *Environ. Sci. Technol.* 45, 3710–3717.
- Railsback, S.F., Grimm, V., 2011. Agent-Based and Individual-Based Modeling: A Practical Introduction. Princeton University Press, New Jersey, USA.
- Ramkrishna, D., Song, H.-S., 2012. Dynamic models of metabolism. A review of the cybernetic approach. *Am. Inst. Chem. Eng. J.* 58, 986–997.
- Rinke, K., Petzoldt, T., 2003. Modelling the effects of temperature and food on individual growth and reproduction of *Daphnia* and their consequences on the population level. *Limnologia* 33, 293–304.
- Sarnelle, O., 2005. *Daphnia* as keystone predators: effects on phytoplankton diversity and grazing resistance. *J. Plankton Res.* 27, 1229–1238. <http://dx.doi.org/10.1093/plankt/fbi086>.
- Scheffer, M., Rinaldi, S., Kuznetsov, Y.A., 2000. Effects of fish on plankton dynamics: a theoretical analysis. *Can. J. Fish. Aquat. Sci.* 57, 1208–1219.
- Scheffer, M., Carpenter, S., Foley, J.A., Folke, C., Walker, B., 2001. Catastrophic shifts in ecosystems. *Nature* 413, 591–596.
- Schoener, T.W., 2009. The niche. In: Levin, S. (Ed.), Princeton Guide to Ecology. Princeton University Press, Princeton, New Jersey, pp. 3–13.
- Sousa, T., Domingos, T., Kooijman, S.A.L.M., 2008. From empirical patterns to theory: a formal metabolic theory of life. *Philos. Trans. R. Soc. Lond. Ser. B Biol. Sci.* 363, 2453–2464. <http://dx.doi.org/10.1098/rstb.2007.2230>.
- Sousa, T., Domingos, T., Poggiale, J.-C., Kooijman, S.A.L.M., 2010. Dynamic energy budget theory restores coherence in biology. *Philos. Trans. R. Soc. Lond. Ser. B Biol. Sci.* 365, 3413–3428. <http://dx.doi.org/10.1098/rstb.2010.0166>.
- Sterner, R.W., 1990. The ratio of nitrogen to phosphorus resupplied by herbivores: zooplankton and the algal competitive arena. *Am. Nat.* <http://dx.doi.org/10.1086/285092>.
- Sterner, R.W., Elser, J.J., 2002. Ecological Stoichiometry: The Biology of Elements from Molecules to the Biosphere. Princeton University Press, New Jersey, USA.
- Taylor, N.S., Weber, R.J.M., Southam, A.D., Payne, T.G., Hrydziusko, O., Arvanitis, T.N., Viant, M.R., 2009. A new approach to toxicity testing in *Daphnia magna*: application of high throughput FT-ICR mass spectrometry metabolomics. *Metabolomics* 5, 44–58.
- Taylor, N.S., Weber, R.J.M., White, T.A., Viant, M.R., 2010. Discriminating between different acute chemical toxicities via changes in the daphnid metabolome. *Toxicol. Sci.* 118, 307–317. <http://dx.doi.org/10.1093/toxsci/kfq247>.

- Vandenbrouck, T., Jones, O.A.H., Dom, N., Griffin, J.L., De Coen, W., 2010. Mixtures of similarly acting compounds in *Daphnia magna*: from gene to metabolite and beyond. *Environ. Int.* 36, 254–268. <http://dx.doi.org/10.1016/j.envint.2009.12.006>.
- Viant, M.R., 2008. Recent developments in environmental metabolomics. *Mol. BioSyst.* 4, 980–986. <http://dx.doi.org/10.1039/b805354e>.
- Wagner, N.D., Lankadurai, B.P., Simpson, M.J., Simpson, A.J., Frost, P.C., 2015. Metabolomic differentiation of nutritional stress in an aquatic invertebrate. *Physiol. Biochem. Zool.* 88, 43–52. <http://dx.doi.org/10.1086/679637>.
- Wangersky, P.J., 1978. Lotka-Volterra population models. *Annu. Rev. Ecol. Syst.* 9, 189–218.
- Wiener, N., 1947. A scientist rebels. *Atl. Mon.* 179, 46.

**USING DAPHNIA PHYSIOLOGY TO DRIVE FOOD WEB DYNAMICS: A
THEORETICAL REVISIT OF LOTKA-VOLTERRA MODELS**

(SUPPORTING INFORMATION)

**Gurbir Perhar, Noreen E. Kelly, Felicity J. Ni, Myrna J. Simpson, Andre J.
Simpson, George B. Arhonditsis***

Department of Physical and Environmental Sciences, University of Toronto.
1265 Military Trail, Scarborough, Ontario, M1C 1A4, Canada

* Corresponding author

e-mail: georgea@utsc.utoronto.ca, Tel.: +1 416 208 4858; Fax: +1 416 287 7279

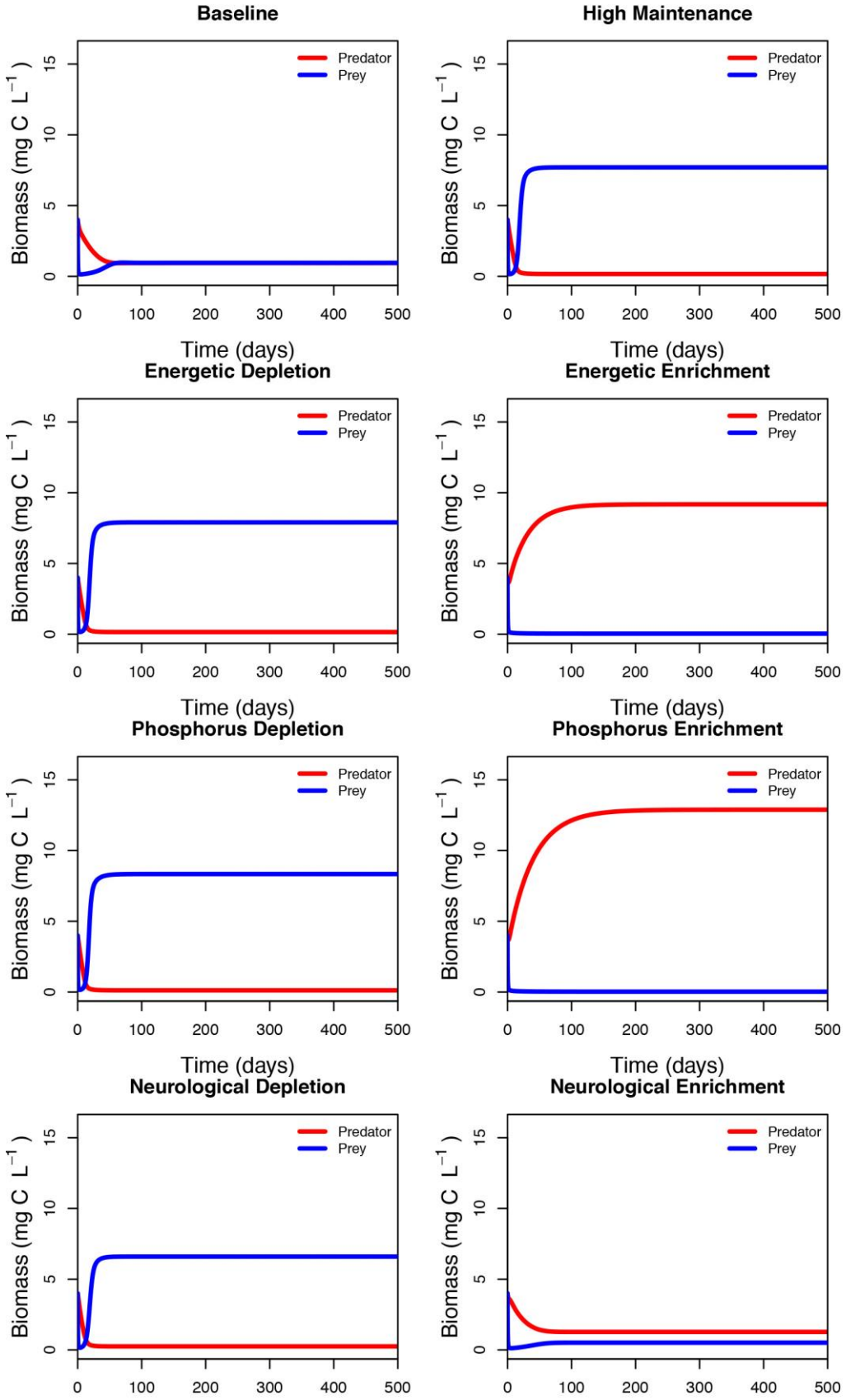
Table S1: Parameter descriptions and values pertaining to *Daphnia* physiology sub-model of Perhar and Arhonditsis (2015), and the Lotka-Volterra predator-prey model, used in this study.

Symbol	Value	Unit	Equation from Table 2	Definition
TRY_{som}	21.7	$\mu\text{g TRY mg C}^{-1}$	5, 6	Somatic tryptophan to carbon ratio
TYR_{som}	23.7	$\mu\text{g TYR mg C}^{-1}$	5, 6	Somatic tyrosine to carbon ratio
$CARB_{som}$	130	$\mu\text{g CARB mg C}^{-1}$	5, 6	Somatic carbohydrate to carbon ratio
FAT_{som}	131	$\mu\text{g FAT mg C}^{-1}$	5, 6	Somatic saturated fatty acid to carbon ratio
$PROT_{som}$	158	$\mu\text{g PROT mg C}^{-1}$	5, 6	Somatic protein to carbon ratio
CLS_{som}	25.3	$\mu\text{g CLS mg C}^{-1}$	5, 6	Somatic cholesterol to carbon ratio
CHO_{som}	9.69	$\mu\text{g CHO mg C}^{-1}$	5, 6	Somatic choline to carbon ratio
EPA_{som}	24.6	$\mu\text{g EPA mg C}^{-1}$	5, 6	Somatic eicosapentaenoic acid to carbon ratio
DHA_{som}	2.8	$\mu\text{g DHA mg C}^{-1}$	5, 6	Somatic docosahexaenoic acid to carbon ratio
GLY_{som}	5.16	$\mu\text{g GLY mg C}^{-1}$	5, 6	Somatic glycine to carbon ratio
GA_{som}	43.1	$\mu\text{g GA mg C}^{-1}$	5, 6	Somatic glutamic acid to carbon ratio
CYS_{som}	17.3	$\mu\text{g CYS mg C}^{-1}$	5, 6	Somatic cysteine to carbon ratio
P_{som}	8.74	$\mu\text{g P mg C}^{-1}$	5, 6	Somatic phosphorus to carbon ratio
N_{som}	77.9	$\mu\text{g N mg C}^{-1}$	5, 6	Somatic nitrogen to carbon ratio
<i>Low</i>	0.109	unitless	5	Lower fraction for calculating minimum somatic congener bounds
<i>High</i>	1.18	unitless	6	Upper fraction for calculating optimum somatic congener bounds
α_{c1}	0.9	unitless	1	Thermodynamic constraint 1
α_{c2}	0.03	$(\text{mg C L}^{-1})^{1/2}$	1	Thermodynamic constraint 2
FQ	0.647	$(\text{mg C L}^{-1})^{1/2}$	1	Food quality index
G_{max}	0.64	day^{-1}	42	Maximum zooplankton growth rate
E_{hs}	0.45	$\text{J mg C}^{-1} \text{day}^{-1}$	42	Use efficiency of energy allocated to anabolism and reproduction
<i>b</i>	5	unitless	28	Sets the supersaturation level in which the turnover begins
<i>c</i>	2	unitless	28	Increase of turnover rate with increasing supersaturation
<i>top</i>	0.25	unitless	28	Maximum fraction of growth energy diverted to homeostatic turnover
N_{NEURO}	0.5	unitless	10	Fraction of nitrogen for neurotransmitter synthesis
N_{ANA}	0.5	unitless	37	Fraction of nitrogen for growth
P_{ENERGY}	0.33	unitless	17, 18	Fraction of phosphorus for energetics
P_{MAINT}	0.33	unitless	22	Fraction of phosphorus for maintenance
P_{ANA}	0.33	unitless	36	Fraction of phosphorus for growth
FAT_{ENERGY}	0.5	unitless	13	Fraction of fat for energetics
FAT_{MAINT}	0.5	unitless	25	Fraction of fat for maintenance
CLS_{MAINT}	0.5	unitless	24	Fraction of cholesterol for maintenance
CLS_{ANA}	0.5	unitless	38	Fraction of cholesterol for growth
EC_{brkd_1}	0.1	unitless	20	Fraction of total energy for maintenance
EC_{brkd_2}	0.435	unitless	33	Fraction of total energy for anabolism

EC_{brkd_3}	0.565	unitless	34	Fraction of total energy for reproduction
OSM_{brkd_1}	0.25	unitless	22	Fraction of maintenance energy allotted to phosphorus
OSM_{brkd_2}	0.25	unitless	23	Fraction of maintenance energy allotted to choline
OSM_{brkd_3}	0.25	unitless	24	Fraction of maintenance energy allotted to cholesterol
OSM_{brkd_4}	0.25	unitless	25	Fraction of maintenance energy allotted to fat
WAS_{brkd_1}	0.33	unitless	29	Fraction of waste management energy allotted to glycine
WAS_{brkd_2}	0.33	unitless	30	Fraction of waste management energy allotted to glutamic acid
WAS_{brkd_3}	0.33	unitless	31	Fraction of waste management energy allotted to cysteine
ANA_{brkd_1}	0.33	unitless	36	Fraction of anabolic energy allotted to phosphorus
ANA_{brkd_2}	0.33	unitless	37	Fraction of anabolic energy allotted to nitrogen
ANA_{brkd_3}	0.33	unitless	38	Fraction of anabolic energy allotted to cholesterol
REP_{brkd_1}	0.5	unitless	40	Fraction of reproductive energy allotted to EPA
REP_{brkd_2}	0.5	unitless	41	Fraction of reproductive energy allotted to DHA
$NeuroRate$	0.171	day ⁻¹	8, 9, 10	Neurological congener mobilization rate
$MobRate$	0.242	day ⁻¹	11, 13, 15, 17	Energetic congener mobilization rate
$CARB_{YIELD}$	0.0167	J μg CARB ⁻¹	12	Energetic yield of carbohydrates
FAT_{YIELD}	0.0377	J μg FAT ⁻¹	14	Energetic yield of fat
$PROT_{YIELD}$	0.0167	J μg PROT ⁻¹	16	Energetic yield of protein
$TRY_{A.E.}$	$7.05 \cdot 10^{-4}$	J μg TRY ⁻¹	28	Tryptophan activation energy
$TYR_{A.E.}$	$7.06 \cdot 10^{-4}$	J μg TYR ⁻¹	28	Tyrosine activation energy
$CARB_{A.E.}$	$5.65 \cdot 10^{-4}$	J μg CARB ⁻¹	28	Carbohydrate activation energy
$FAT_{A.E.}$	$3.16 \cdot 10^{-4}$	J μg FAT ⁻¹	25, 28	Fat activation energy
$PROT_{A.E.}$	$2.81 \cdot 10^{-4}$	J μg PROT ⁻¹	28	Protein activation energy
$CLS_{A.E.}$	$1.90 \cdot 10^{-5}$	J μg CLS ⁻¹	24, 28, 38	Cholesterol activation energy
$CHO_{A.E.}$	$7.99 \cdot 10^{-4}$	J μg CHO ⁻¹	23, 28	Choline activation energy
$EPA_{A.E.}$	$1.36 \cdot 10^{-4}$	J μg EPA ⁻¹	28, 40	EPA activation energy
$DHA_{A.E.}$	$1.12 \cdot 10^{-4}$	J μg DHA ⁻¹	28, 41	DHA activation energy
$CYS_{A.E.}$	$7.28 \cdot 10^{-4}$	J μg CYS ⁻¹	28, 31	Cysteine activation energy
$GLY_{A.E.}$	$5.31 \cdot 10^{-4}$	J μg GLY ⁻¹	28, 29	Glycine activation energy
$GA_{A.E.}$	$3.03 \cdot 10^{-4}$	J μg GA ⁻¹	28, 30	Glutamic acid activation energy
$P_{A.E.}$	$1.29 \cdot 10^{-3}$	J μg P ⁻¹	22, 28, 36	Phosphorus activation energy
$N_{A.E.}$	$2.49 \cdot 10^{-3}$	J μg N ⁻¹	28, 37	Nitrogen activation energy

Table S2: Algal congener concentrations for the baseline scenario.

<i>SYMBOL</i>	<i>DESCRIPTION</i>	<i>VALUE</i>	<i>UNIT</i>
ALGAL _{TRY}	Algal tryptophan to carbon ratio	12.9	μg TRY mg C ⁻¹
ALGAL _{TYR}	Algal tyrosine to carbon ratio	15.375	μg TYR mg C ⁻¹
ALGAL _{CARB}	Algal carbohydrate to carbon ratio	79.5	μg CARB mg C ⁻¹
ALGAL _{FAT}	Algal fat to carbon ratio	64.5	μg FAT mg C ⁻¹
ALGAL _{PROT}	Algal protein to carbon ratio	115	μg PROT mg C ⁻¹
ALGAL _{CLS}	Algal cholesterol to carbon ratio	9	μg CLS mg C ⁻¹
ALGAL _{CHO}	Algal choline to carbon ratio	2.9	μg CHO mg C ⁻¹
ALGAL _{EPA}	Algal EPA to carbon ratio	4.47	μg EPA mg C ⁻¹
ALGAL _{DHA}	Algal DHA to carbon ratio	1.47	μg DHA mg C ⁻¹
ALGAL _{CYS}	Algal cysteine to carbon ratio	5.1	μg CYS mg C ⁻¹
ALGAL _{GA}	Algal glutamic acid to carbon ratio	11.8	μg GA mg C ⁻¹
ALGAL _{GLY}	Algal glycine to carbon ratio	1.62	μg GLY mg C ⁻¹
ALGAL _P	Algal phosphorus to carbon ratio	4.5	μg P mg C ⁻¹
ALGAL _N	Algal nitrogen to carbon ratio	36.05	μg N mg C ⁻¹



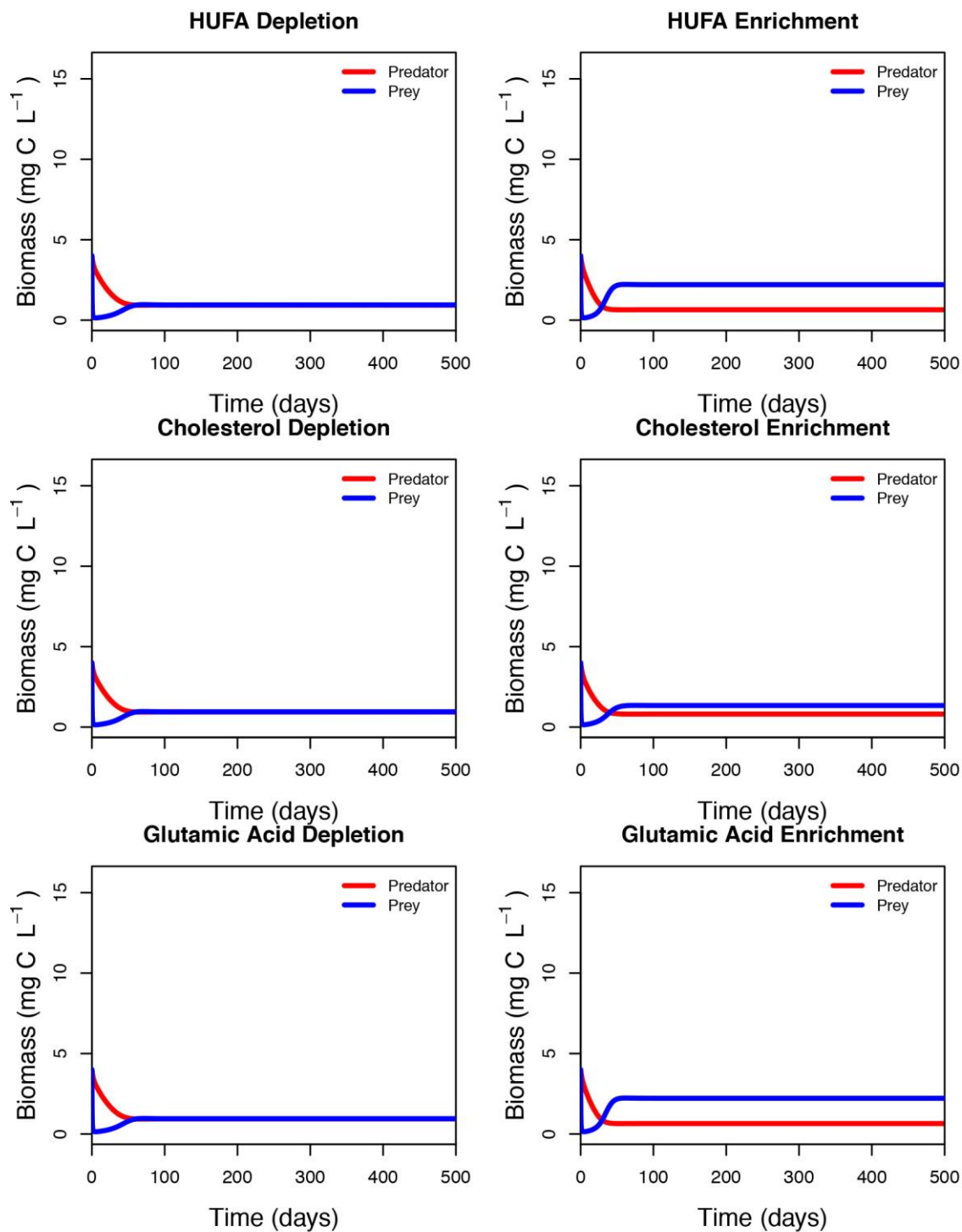


Figure S1. Predator (red) and prey (blue) biomass (mg C L⁻¹) trajectories under different algal nutritional enrichment and depletion scenarios. The corresponding daily energetic signatures for each scenario are presented in Table 4.